

The universal vibrational dynamics of water bound to tertiary amines: More than just Fermi resonance ESI

Eaindra Lwin, Nils O. B. Lüttchwager, Martin A. Suhm*

*Institute of Physical Chemistry, University of Göttingen, Tammannstr. 6, 37077 Göttingen
(Germany). E-mail: msuhm@gwdg.de*

Note: The supplement is a collection of 3 different documents, labelled Part 1 to 3. Be sure to scroll past the references of Part 1 to find the remaining two parts. Part 2 explains the algorithm used to derive coupling elements and deperturbed positions (Julia package “Fermi4x4”), Part 3 shows the data evaluation notebook which uses Fermi4x4 to derive the deperturbation results presented in the main paper.

Part 1: Supplementary Figures and Tables

Contents

1 Experiment	S3
1.1 Investigated compounds	S3
1.2 Experimental details	S3
2 Individual band centers and intensities from experimental spectra	S6
2.1 Method I	S6
2.2 Method II	S6
2.3 Method III	S6
2.4 Method IV	S6
3 Harmonic modeling	S9
3.1 Details on harmonic calculations	S9
4 Four anharmonic coupling models	S12
5 Isotope effect in the monohydrates of tertiary amines	S14
6 Perturbed and deperturbed ON stretching vibration in models C and C'	S20
7 Quantum chemical bridging	S22
8 Methylation instead of deuteration	S24
9 Dihydrate contributions to the HyDRA database	S26
10 Experimental spectra of triisopropylamine (IIIN)	S30
11 Example inputs for transition states	S32
References	S33

List of Tables

S1 Table of investigated compounds	S3
S2 Experimental details for the FTIR spectra in the main text and supplementary information	S4
S3 Experimental details for the Raman spectra in the main text and supplementary information	S5
S4 Experimental band centers for the resonance tetrad	S7
S5 Experimental intensities for the resonance tetrad	S8
S6 Harmonic prediction of OHb, b2, b2ON, b2ON2 and OHbON for amine monohydrates	S9

S7	Relative energy for two different conformers of MMIN and its monohydrate	S10
S8	Relative energy for two different conformers of MMCN and its monohydrate	S11
S9	Coupling constants and deperturbed positions using coupling model A	S13
S10	Coupling constants and deperturbed positions using coupling model B	S13
S11	Deperturbed positions using coupling model C	S13
S12	Coupling constants using coupling model C	S13
S13	Experimental and harmonic H/D isotope effect on OHb for tertiary amine monohydrates	S15
S14	Raw and different deperturbed OHb wavenumbers for tertiary amine monohydrates	S16
S15	Experimental ^{16/18} O isotope effects on OHb wavenumbers of tertiary amine monohydrates	S20
S16	Raw and deperturbed wavenumbers by applying model C for ON and 2ON	S20
S17	Anharmonicity constants by applying model C for ON and 2ON	S21
S18	Raw and deperturbed wavenumbers by applying model C' for ON	S21
S19	Relative energy for three different conformers of EEEN monomer using B3LYP-D3/def2-TZVP	S22
S20	Relative energy for three different conformers of EEEN monohydrate using B3LYP-D3/def2-TZVP	S22
S21	Harmonic and deperturbed wavenumbers of EEEN monohydrates by using coupling model C	S23
S22	Perturbed wavenumbers and intensities of EEEN monohydrates by using coupling model C	S23
S23	Harmonic and deperturbed wavenumbers of EEEN monohydrates by using coupling model C'	S23
S24	Perturbed wavenumbers and intensities of EEEN monohydrates by using coupling model C'	S23
S25	Harmonic ON and OHb wavenumbers in complexes of tertiary amines with MeOH	S24
S26	Hydrogen bond torsion angles in complexes of amines with water and methanol	S25
S27	Example input for NEB scan	S32
S28	Example input for transition state calculation	S32

List of Figures

S1	Two conformers of N,N-dimethylisopropylamine (MMIN) monomer and its monohydrate	S10
S2	Two conformers of N,N-dimethylcyclohexylamine (MMCN) monomer and its monohydrate	S11
S3	Coupling model A	S12
S4	Coupling model B	S12
S5	Coupling model C	S12
S6	Coupling model C'	S12
S7	Cold spectra of MN4 with HOH and DOH	S14
S8	Cold spectra of MMCN with HOH and DOH	S15
S9	Cold spectra of MMTN with HOH and DOH	S16
S10	Cold Raman spectra of MMTN with HOH and FTIR spectra with DOH	S17
S11	Comparison of FTIR and Raman spectra for the monohydrate of MMTN	S18
S12	Cold spectra for isotope substitution of water with tertiary amines	S19
S13	Cold spectra of MN5 with ¹⁶ OH ₂ and ¹⁸ OH ₂	S19
S14	Three conformers of triethylamine (EEEN) monohydrate	S22
S15	Illustration of the torsion angle of water and methanol docking to an amine	S24
S16	Spectra for MN4+HOH, MN4+DOH and MN4+MeOH	S25
S17	Dihydrate spectra of MN5	S26
S18	Dihydrate spectra of MMCN	S27
S19	Dihydrate spectra of MMTN	S28
S20	Dihydrate spectra of N555	S29
S21	Dihydrate spectra of IIIN	S30
S22	Spectral comparison of IIIN and MN5MMMM with water	S31
S23	Spectral comparison of IIIN and MMCN with water	S31

1 Experiment

1.1 Investigated compounds

Table S1 gives details about the studied chemicals and introduces their codes (acronyms) used in the main document.

Table S1: Table of employed chemicals, their code names (supplement and main document), their CAS number, the supplier, purity and Lot#.

Name	Code	CAS Number	Supplier	Purity	Lot#
N-Methylpyrrolidine	MN4	120-94-5	TCI	98%	QV5SL-KH
N-Methylpiperidine	MN5	626-67-5	TCI	99%	BK82C-SY
1-Azabicyclooctane	N555	100-76-5	BLDpharm	98%	-
1,2,2,6,6-Pentamethylpiperidine	MN5MMMM	79-55-0	BLDpharm	99.85%	DRX383
N,N-Dimethylethylamine	MMEN	598-56-1	TCI	98%	PV8KA-UD
N,N-Dimethylisopropylamine	MMIN	996-35-0	TCI	99%	FGI01-CI
N,N-Dimethylcyclohexylamine	MMCN	98-94-2	TCI	98%	A6M8I-OH
<i>tert</i> -Butyldimethylamine	MMTN	918-02-5	Angene	97%	AGN23-1430724-1
Triethylamine	EEEN	121-44-8	TCI	99%	JUJ3F-TU
Triisopropylamine	IIIN	3424-21-3	ChemCruz	-	K2223
Methanol	MeOH	67-56-1	TCI	99.8%	NOSCB-PS
Demineralised water	H ₂ O	7732-18-5	-	-	-
Deuterated water	D ₂ O	7789-20-0	Abcr	99.85%	AB-403423
Helium	He	7440-59-7	Nippon	99.996%	-
Neon	Ne	7440-59-7	Linde	99.999%	-

1.2 Experimental details

All FTIR spectra were obtained using the *gratin* jet spectrometer (for a detailed description see [1]) and important parameters for the recorded spectra can be found in Table S2. The spectral traces in the range of 4000 - 2200 cm⁻¹ are provided here: dataset.

Details of the experimental setup for the Raman measurements are given in [2] and more information on the recorded Raman spectra can be found in Table S3. All Raman experimental spectra in the range of 4000 - 2200 cm⁻¹ are also provided here: dataset.

Table S2: Spectroscopic details of FTIR spectra shown in Figs. 1, 2, 4, 5, 6, 10, 11 and 12 from the main text and Figs. S7, S8, S9, S10, S11, S12, S13, S16, S17, S18, S19, S20, S21, S22, S23 from the ESI. The partial pressures of the amine (p_A), the solvent (p_S) such as water H_2O , deuterated water D_2O or methanol $MeOH$, as well as the carrier gases helium (p_{He}) or neon (p_{Ne}) and the total stagnation pressure of the expansion (p_s) are given. The background pressure in the buffer chamber oscillates between about 0.01 and 0.1 hPa for Ne. The spectra were obtained by averaging # FTIR scans, each synchronized to a 133 ms gas pulse through a 700 mm \times 0.2 mm slit nozzle with a Bruker VERTEX 70v FTIR spectrometer in double-sided mode at 140 kHz scanning speed. A 20 W tungsten light source, an InSb/HgCdTe sandwich detector and an optical filter (wavenumber range $<4000\text{ cm}^{-1}$) were used. The recording date of the spectra is given in a dd/mm/yyyy format and the last column is indicated in which figures in the main publication and the ESI, the corresponding spectrum is shown.

p_A /hPa	p_S /hPa	p_{He} /hPa	p_{Ne} /hPa	p_s /hPa	#	dd/mm/yyyy	Figure
MMEN	H_2O						
0.2	0.4	749	0	750	700	30/10/2023	6,12
MN4							
0.2	0.4	749	0	750	1000	27/07/2023	4,12,S7, S16
N555							
0.1	0.4	749	0	750	800	12/06/2023	5,12S20
0.1	0.1	750	0	750	800	31/05/2023	S20
MN5							
0.2	0.4	749	0	750	800	28/06/2023	1,12,S13,S17
0.2	0.0	750	0	750	800	26/06/2023	S17
MMIN							
0.2	0.4	749	0	750	900	16/11/2023	6,12
MMCN							
0.2	0.2	750	0	750	1000	04/07/2023	6,12,S8,S18, S23
0.2	0.0	750	0	750	1000	03/07/2023	S18
MMTN							
0.1	0.2	0	400	400	800	16/10/2024	6,12,S9,S11,S19
0.2	0.2	750	0	750	800	29/01/2024	S19
MN5MMMM							
0.2	0.4	749	0	750	800	21/02/2024	2,12
EEEN							
0.2	0.4	749	0	750	1000	13/09/2023	10
IIN							
0.2	0.7	749	0	750	2000	22+25/01/2024	S21,S22, S23
0.2	0.4	749	0	750	2000	22/01/2024	S21
MN4	D_2O						
0.2	0.4	0	399	400	200	08/04/2024	S7,S16
MN5							
0.2	0.8	749	0	750	700	08/08/2023	1, S12
MMCN							
0.2	0.8	749	0	750	400	11/08/2023	S8
MMTN							
0.2	0.4	0	399	400	500	21/03/2024	S9, S10
MN5MMMM							
0.2	0.4	0	399	400	500	20/03/2024	2,S12
N555	$^{18}OH_2$						
0.1	0.4	750	0	750	800	13/06/2023	5
MN5							
0.2	0.4	749	0	750	1000	24/10/2023	S13
MN4	$MeOH$						
0.2	0.1	0	400	400	500	28/06/2024	11,S16
MMCN							
0.1	0.1	0	400	400	700	18/10/2024	11
MMTN							
0.2	0.2	0	400	400	500	31/05/2024	11
MN5MMMM							
0.2	0.2	0	400	400	500	10/05/2024	11

Table S3: Details of the Raman spectra in Fig. 4 from the main text and Figs. S10 and S11 from the ESI. Column labels have the same meaning as in Table S2. Note that since the Raman jet-setup probes a continuous expansion, but the FTIR jet-setup probes pulses, and gas is filled in the full vacuum part of the Raman setup (with the circulation switched off) but only in the reservoir of the FTIR setup when preparing the gas samples, the stagnation pressure p_s and carrier gas partial pressure $p_{\text{He/Ne}}$ are almost identical in case of FTIR measurements, but quite distinct for Raman measurements. Additional columns in this table are: p_0 — background pressure in expansion chamber, T — overall exposure time. MN4 spectra were recorded at a nozzle distance of 1 mm, MMTN spectra at 2 mm. The laser output power was set between 18 and 20 W.

p_A/hPa	p_w/hPa	p_{He}/hPa	p_{Ne}/hPa	p_s/hPa	p_0/hPa	T/h:min	dd/mm/yyyy	Figure
MN4	H ₂ O							
0.1	>0.2	—	90	500	6	1:30	06/02/2024	4
0.4	—	—	90	500	6	0:35	05/02/2024	4
MMTN								
0.2	0.4	100	—	500	9	5:20	12/03/2024	S10,S11
0.4	—	100	—	500	9	2:20	18/03/2024	S10,S11

2 Individual band centers and intensities from experimental spectra

To determine the deperturbed positions D of b2, OHb, b2ON and xONn and the coupling constants W between them by using different models as described in the main text, the individual experimental band centers and intensities have to be extracted. The spectra in the range 3050 - 3550 cm^{-1} as shown in Fig. 12 of the main text are evaluated by integrating the area I under the individual bands, also resulting in individual uncertainties ΔI . The center $\tilde{\nu}$ of a band system is taken as the intensity center or center of gravity and has an uncertainty $\Delta\tilde{\nu}$. It is usually close to the intensity maximum of the individual band.

I and $\tilde{\nu}$ are estimated based on four different integration methods for the individual areas I . The four integration methods (I, II, III, IV) are described in detail below. The resulting band centers $\tilde{\nu}$ and intensities I as well as their uncertainties $\Delta\tilde{\nu}$ and ΔI of each method for the four bands (b2, OHb, b2ON and xONn) are given in Table S4 and S5. All four methods are largely based on the NoisySignalIntegration method by Nils O. B. Lüttschwager [3], which allows for different settings of the integration windows. Briefly, the program analyzes the actual noise of the spectrum in a given wavenumber range and uses this noise to simulate alternative noise with the same characteristics to a sample before the integration is performed.

The averages of the individual intensities \bar{I} and of the band centers $\bar{\nu}$ from the four independent integration methods are also listed in Table S4 and S5 and are our best estimates of the true values. An estimate of their uncertainties $\Delta\Delta I$ and $\Delta\Delta\tilde{\nu}$ is obtained by determining the combined spread of the individual likelihood histograms near the 25% threshold. This would correspond to about 90% confidence (1.66σ) for a Gaussian distribution.

2.1 Method I

A narrow integration window which is approximately centering the highest peak position of the band is chosen so that the signal remains consistently above the noise level. The integration boundaries (start and end point of the integration window) are allowed to vary by 1 cm^{-1} . To give an example for the OHb band of the MMEN monohydrate which has the highest peak position at 3301 cm^{-1} , the low integration boundary is selected in the 3285-3286 cm^{-1} range and the high boundary in the 3316-3317 cm^{-1} range.

2.2 Method II

A wider integration window is selected which extends significantly into the noisy baseline. At the same time, the integration start and end points are allowed to vary more strongly by 3 cm^{-1} . In the MMEN example, the boundaries are chosen from the ranges 3282-3285 cm^{-1} and 3317-3320 cm^{-1} .

2.3 Method III

The integration boundaries are allowed to vary over the combined ranges of methods I and II. Staying with the MMEN example, the integration is carried out from 3282-3286 cm^{-1} to 3316-3320 cm^{-1} .

2.4 Method IV

The integration is based on a symmetric window where the start and end points have the same distance to the band maximum. The variability of the window width is chosen such that the start and end point vary by approximately 5 cm^{-1} . For the main band of MMEN, the maximum position is at 3301 cm^{-1} and the sampled integration window ranges from 3284-3289 cm^{-1} to 3313-3318 cm^{-1} .¹

¹In NoisySignalIntegration, for Methods I to III, the integration window was specified using two uniform distributions to define the start and end point, both spanning 1 cm^{-1} (Method I), 3 cm^{-1} (Method II), and 4 cm^{-1} (Method III). For Method IV, the integration window was specified using one uniform distribution (spanning 10 cm^{-1}) for the width of the band and the peak position, which leads to symmetric integration around the central peak of the band.

Table S4: Experimental band centers $\tilde{\nu}$ and their uncertainties $\Delta\tilde{\nu}$ of four integration methods as well as average band centers $\bar{\tilde{\nu}}$ and their uncertainties $\Delta\Delta\tilde{\nu}$ for b2, OHb, b2ON and xONn of amine-water complexes. All values are in cm^{-1} .

Code	I		II		III		IV		$\bar{\tilde{\nu}}$	$\Delta\Delta\tilde{\nu}$
	$\tilde{\nu}$	$\Delta\tilde{\nu}$	$\tilde{\nu}$	$\Delta\tilde{\nu}$	$\tilde{\nu}$	$\Delta\tilde{\nu}$	$\tilde{\nu}$	$\Delta\tilde{\nu}$		
MMEN										
b2	3191.38	0.087	3191.37	0.124	3191.37	0.102	3191.44	0.26	3191.39	0.325
OHb	3300.95	0.145	3300.9	0.147	3300.91	0.131	3301.02	0.0981	3300.945	0.22
b2ON	3351.4	0.266	3351.78	0.287	3351.65	0.25	3351.56	0.268	3351.5975	0.5625
xONn	3447.07	0.47	3447.39	0.599	3447.4	0.589	3443.94	5.63	3446.45	2.0625
MN4										
b2	3190.54	0.17	3191.32	0.261	3191.05	0.224	3190.36	0.266	3190.8175	0.85
OHb	3299.11	0.147	3299.19	0.158	3299.16	0.138	3299.33	0.114	3299.1975	0.29
b2ON	3347.51	0.206	3347.57	0.224	3347.55	0.198	3347.72	0.306	3347.5875	0.45
xONn	3441.7	0.628	3440.89	0.8	3441.14	0.662	3441.79	2.36	3441.38	1
N555										
b2	3193.06	0.0865	3193.36	0.19	3193.21	0.123	3193.44	0.188	3193.2675	0.36
OHb	3296.84	0.337	3296.81	0.355	3296.82	0.308	3296.29	0.229	3296.69	0.66
b2ON	3351.42	0.236	3351.05	0.303	3351.19	0.253	3351.1	0.193	3351.19	0.5
xONn	3439.74	0.719	3441.24	0.712	3440.74	0.627	3440.5	0.775	3440.555	1.65
MN5										
b2	3188.11	0.159	3189.49	0.27	3188.89	0.225	3188.35	0.233	3188.71	0.94
OHb	3289.29	0.133	3289.6	0.192	3289.49	0.126	3289.18	0.146	3289.39	0.405
b2ON	3342.28	0.113	3342.16	0.198	3342.18	0.143	3342.44	0.244	3342.265	0.435
xONn	3429.2	0.537	3429.6	0.655	3429.52	0.56	3429.66	1.15	3429.495	1.5
MMIN										
b2	3187.08	0.142	3186.99	0.153	3187.02	0.133	3186.82	0.121	3186.9775	0.3
OHb	3284.89	0.127	3284.75	0.135	3284.8	0.118	3284.42	0.161	3284.715	0.43
b2ON	3347.88	0.131	3348.13	0.167	3348.05	0.141	3347.99	0.145	3348.0125	0.31
xONn	3430.8	0.619	3430.07	0.466	3430.23	0.44	3431.29	1.29	3430.5975	1.4
MMCN										
b2	3186.19	0.114	3185.94	0.146	3186.07	0.119	3186.06	0.0858	3186.065	0.25
OHb	3282.02	0.198	3282.11	0.203	3282.07	0.172	3281.87	0.131	3282.0175	0.3
b2ON	3347.14	0.155	3347.38	0.354	3347.01	0.193	3346.94	0.233	3347.1175	0.6
xONn	3426.79	0.405	3426.48	0.367	3426.48	0.369	3426.83	0.457	3426.645	0.7
MMTN										
b2	3180.19	0.0654	3180.35	0.0764	3180.29	0.0874	3180.24	0.0559	3180.2675	0.16
OHb	3270.3	0.301	3270.98	0.273	3270.8	0.245	3269.04	0.0988	3270.28	0.695
b2ON	3344.07	0.165	3344.35	0.202	3344.26	0.162	3343.76	0.213	3344.11	0.55
xONn	3414.62	0.33	3414.59	0.417	3414.6	0.346	3416.18	0.903	3414.9975	1.49
MN5MMMM										
b2	3176.32	0.183	3176.13	0.186	3176.19	0.164	3176.02	0.105	3176.165	0.31
OHb	3257.51	0.2	3257.55	0.202	3257.54	0.179	3257.23	0.131	3257.4575	0.365
b2ON	3335.17	0.514	3334.74	0.464	3334.88	0.422	3332.04	0.35	3334.2075	2.14
xONn	3393.16	0.352	3393.05	0.401	3393.09	0.342	3393.09	0.643	3393.0975	0.81

Table S5: Experimental IR intensities I and their uncertainties ΔI for four integration methods as well as average intensities \bar{I} and their uncertainties $\Delta\Delta I$ for b2, OHb, b2ON and xONn of amine-water complexes.

Code	I		II		III		IV		\bar{I}	$\Delta\Delta I$
	I	ΔI	I	ΔI	I	ΔI	I	ΔI		
MMEN										
b2	2.14E-04	8.68E-06	2.23E-04	9.71E-06	2.21E-04	8.28E-06	2.59E-04	1.28E-05	2.29E-04	3.45E-05
OHb	7.45E-04	2.12E-05	8.04E-04	2.06E-05	7.88E-04	1.84E-05	7.02E-04	1.44E-05	7.60E-04	7.10E-05
b2ON	2.70E-04	1.70E-05	2.85E-04	1.68E-05	2.81E-04	1.49E-05	2.65E-04	1.41E-05	2.75E-04	2.85E-05
xONn	2.52E-05	5.84E-06	1.78E-05	4.89E-06	1.78E-05	4.89E-06	3.87E-05	1.12E-05	2.49E-05	2.07E-05
MN4										
b2	2.26E-04	1.22E-05	2.10E-04	1.27E-05	2.14E-04	1.12E-05	2.65E-04	1.44E-05	2.29E-04	4.65E-05
OHb	6.97E-04	1.97E-05	7.26E-04	1.91E-05	7.18E-04	1.70E-05	7.28E-04	1.57E-05	7.17E-04	4.25E-05
b2ON	2.15E-04	1.36E-05	2.45E-04	1.38E-05	2.36E-04	1.21E-05	2.24E-04	1.41E-05	2.30E-04	3.35E-05
xONn	4.50E-05	1.01E-05	4.90E-05	1.09E-05	4.79E-05	9.43E-06	2.70E-05	7.00E-06	4.22E-05	2.32E-05
N555										
b2	2.48E-04	9.43E-06	2.49E-04	1.27E-05	2.53E-04	8.57E-06	2.42E-04	1.13E-05	2.48E-04	1.90E-05
OHb	4.94E-04	2.52E-05	4.84E-04	2.37E-05	4.87E-04	2.12E-05	4.54E-04	1.71E-05	4.80E-04	4.60E-05
b2ON	1.74E-04	1.28E-05	1.73E-04	1.33E-05	1.73E-04	1.15E-05	1.69E-04	9.61E-06	1.72E-04	1.85E-05
xONn	2.99E-05	8.02E-06	4.49E-05	9.01E-06	4.05E-05	7.77E-06	3.88E-05	8.12E-06	3.85E-05	1.80E-05
MN5										
b2	1.81E-04	1.07E-05	1.82E-04	1.26E-05	1.88E-04	1.03E-05	2.43E-04	1.20E-05	1.99E-04	4.45E-05
OHb	5.72E-04	1.69E-05	5.82E-04	1.79E-05	5.78E-04	1.37E-05	5.83E-04	1.56E-05	5.79E-04	2.25E-05
b2ON	1.16E-04	7.24E-06	1.18E-04	8.60E-06	1.18E-04	7.27E-06	1.38E-04	9.73E-06	1.22E-04	2.25E-05
xONn	4.89E-05	9.34E-06	5.02E-05	9.72E-06	4.89E-05	9.00E-06	4.80E-05	1.07E-05	4.90E-05	1.50E-05
MMIN										
b2	5.76E-04	1.84E-05	6.06E-04	1.80E-05	5.98E-04	1.60E-05	5.79E-04	1.44E-05	5.90E-04	3.50E-05
OHb	1.08E-03	2.40E-05	1.09E-03	2.28E-05	1.09E-03	2.04E-05	1.17E-03	2.33E-05	1.11E-03	7.35E-05
b2ON	3.05E-04	1.29E-05	3.01E-04	1.34E-05	3.02E-04	1.17E-05	3.04E-04	1.13E-05	3.03E-04	1.85E-05
xONn	6.56E-05	1.14E-05	9.70E-05	1.21E-05	8.79E-05	1.05E-05	5.27E-05	9.69E-06	7.58E-05	3.70E-05
MMCN										
b2	3.57E-04	1.28E-05	4.10E-04	1.45E-05	3.92E-04	1.14E-05	3.74E-04	9.81E-06	3.83E-04	4.35E-05
OHb	6.92E-04	2.36E-05	7.65E-04	2.31E-05	7.44E-04	1.97E-05	6.43E-04	1.59E-05	7.11E-04	8.45E-05
b2ON	2.58E-04	1.28E-05	2.85E-04	1.73E-05	2.88E-04	1.11E-05	3.06E-04	1.42E-05	2.84E-04	4.05E-05
xONn	4.77E-05	7.83E-06	5.55E-05	7.84E-06	5.55E-05	7.84E-06	5.63E-05	8.10E-06	5.37E-05	1.40E-05
MMTN										
b2	6.10E-04	1.49E-05	6.40E-04	1.49E-05	6.59E-04	1.60E-05	6.07E-04	1.13E-05	6.29E-04	4.95E-05
OHb	8.32E-04	2.53E-05	7.83E-04	2.38E-05	7.96E-04	2.13E-05	7.65E-04	1.73E-05	7.94E-04	6.25E-05
b2ON	2.53E-04	1.42E-05	2.92E-04	1.49E-05	2.78E-04	1.24E-05	3.04E-04	1.56E-05	2.82E-04	4.95E-05
xONn	5.40E-05	1.02E-05	5.18E-05	1.09E-05	5.26E-05	9.41E-06	6.53E-05	1.11E-05	5.59E-05	2.85E-05
MN5MMMM										
b2	5.79E-04	1.96E-05	6.15E-04	1.92E-05	6.05E-04	1.71E-05	5.66E-04	1.30E-05	5.91E-04	4.25E-05
OHb	5.72E-04	2.15E-05	6.14E-04	2.10E-05	6.03E-04	1.86E-05	5.30E-04	1.42E-05	5.80E-04	6.45E-05
b2ON	2.41E-04	2.04E-05	2.91E-04	1.97E-05	2.77E-04	1.76E-05	2.02E-04	1.41E-05	2.53E-04	6.50E-05
xONn	1.20E-04	1.28E-05	1.32E-04	1.31E-05	1.29E-04	1.14E-05	1.18E-04	1.41E-05	1.25E-04	2.35E-05

3 Harmonic modeling

3.1 Details on harmonic calculations

The monomer structures of the ten tertiary amines MN4, MN5, MN5MMMM, N555, MMEN, MMIN, MMCN, MMTN, EEEN and IIIN were optimized by using three-body-inclusive D3-dispersion-corrected^[4,5] B3LYP with the def2-TZVP basis set^[6-8] (B3LYP/TZ) on ORCA 5.0.3^[9-12] with the keywords ABC DEFGRID3 VERYTIGHTSCF VERYTIGHTOPT FREQ. Then, the water molecule was attached to the minimum structure of tertiary amine monomers using Chemcraft version 1.8 and the generated monohydrates were preoptimized on CREST^[13,14]. After that, all the possible conformers were reoptimized using B3LYP-D3/def2-TZVP on ORCA 5.0.3 with the same keywords used for the monomers.

For 7 out of the 10 tertiary amines (MN4, MN5, MN5MMMM, N555, MMEN, MMTN and IIIN) one stable monomer conformation was identified, as for their heterodimers with water. The resulting optimized monomer and monohydrate structures of MN4, MN5, MN5MMMM, N555, MMEN, MMTN and IIIN using B3LYP-D3/def2-TZVP on ORCA 5.0.3 are provided here: dataset.

For N,N-dimethylisopropylamine (MMIN), there are two low-lying monomer structures: MMIN_a and MMIN_b, which are shown in Fig. S1. The zero point corrected energy difference ΔE_0 between them is 2.3 kJ/mol, with MMIN_a being more stable. Their 1:1 amine water complexes are close in energy and have similar OH stretching fundamentals, ON stretching fundamentals and bending vibrations of water, all are described in Table S7. Similarly, there are two minimum monomer structures for N,N-dimethylcyclohexylamine (MMCN): MMCN_a and MMCN_b, which are described in Fig. S1. The zero point corrected energy difference ΔE_0 is 2.7 kJ/mol, with MMCN_a being more stable. The zero point corrected energy difference ΔE_0 of their heterodimers is lowered to 1.3 kJ/mol and MMCN_a+H₂O is still the most stable structure, which is described in Table S8. For triethylamine (EEEN), there are three minimum structures for the monomer: EEEN1, EEEN2 and EEEN3. Their optimized structures are shown in Fig. 9 in the main text and their relative energy differences are described in Table S19. Their monohydrates (optimized at B3LYP-D3/def2-TZVP level) are shown in Fig. S14 and their relative energy differences are also described in Table S20. The optimized structures of MMIN, MMCN and EEEN monomers and monohydrates are accessible here: dataset.

To build the mixed trimer structures, a second water molecule was attached to the global minimum structure of the heterodimers using Chemcraft version 1.8, preoptimized using CREST and reoptimized using the same functional and basis set as for monomers and mixed dimers on ORCA 5.0.3.

To build the heterodimers of tertiary amines with methanol, the optimized methanol molecule was attached to the optimized structure of amine monomer, preoptimized using CREST and reoptimized using B3LYP-D3/def2-TZVP on ORCA 5.0.3. The optimized mixed dimer structures are accessible in here: dataset and the harmonic wavenumbers for the OH stretching fundamental OHb and the ON stretching vibrations are described in Table S25.

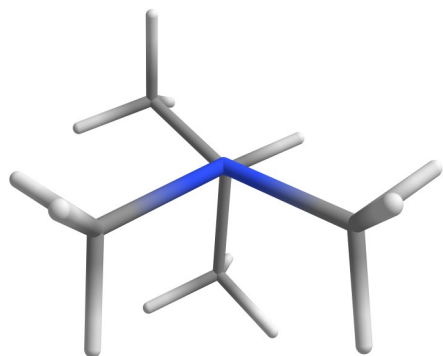
Relevant harmonic wavenumbers ω/cm^{-1} of the 1:1 complexes of 10 tertiary amines with H₂O are shown in Table S6.

Table S6: Harmonic DFT predictions on B3LYP/def2-TZVP level for the ON stretching fundamental ON, its overtone ON2, the bending mode of water b, the bending overtone b2, the OH stretching fundamental OHb, and the combination bands b2ON, b2ON2 and OHbON for 10 amine monohydrates.

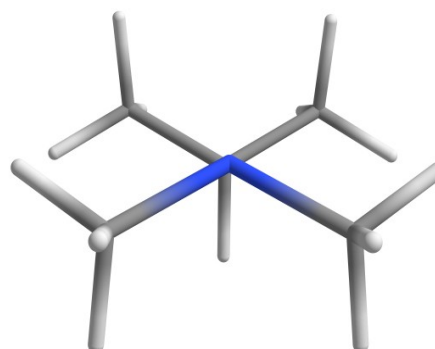
Code	ON	ON2	b	b2	OHb	b2ON	b2ON2	OHbON
MMEN	166	332	1658	3316	3385	3482	3648	3551
MN4	162	324	1656	3312	3384	3474	3636	3546
MMIN_a	165	330	1660	3320	3365	3485	3650	3530
MMIN_b	164	328	1659	3318	3367	3482	3646	3531
MN5	153	306	1657	3314	3370	3467	3620	3523
MMTN	167	334	1663	3326	3342	3493	3660	3509
N555	166	332	1659	3318	3366	3484	3650	3532
MMCN_a	164	328	1661	3322	3366	3486	3652	3530
MMCN_b	165	330	1661	3322	3360	3487	3652	3525
MN5MMMM	161	322	1662	3324	3333	3485	3646	3494
EEEN1	157	313	1660	3320	3377	3477	3633	3533
EEEN2	159	318	1665	3330	3351	3489	3648	3510
EEEN3	163	326	1663	3326	3346	3489	3653	3509
IIIN	119	238	1658	3316	3488	3435	3554	3607

Table S7: Relative electronic ΔE_{el} and zero point corrected ΔE_0 energy of two different monomers of dimethylisopropylamine (MMIN): MMIN_a and MMIN_b and two different heterodimer with water: MMIN_a+H₂O and MMIN_b+H₂O using B3LYP-D3/def2-TZVP. These conformer structures are shown in Fig. S1.

Conformer	$\Delta E_{el}/(\text{kJ/mol})$	$\Delta E_0/(\text{kJ/mol})$	Conformer	$\Delta E_{el}/(\text{kJ/mol})$	$\Delta E_0/(\text{kJ/mol})$
MMIN_a	0	0	MMIN_a+H ₂ O	0	0
MMIN_b	1.6	2.3	MMIN_b+H ₂ O	0.5	1.2



MMIN_a



MMIN_b

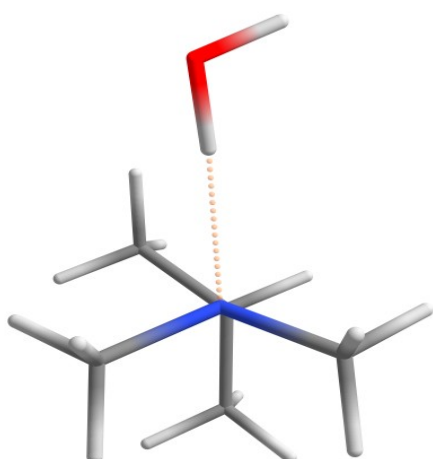
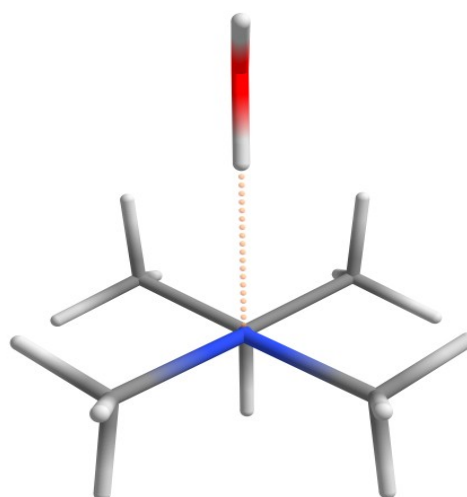
MMIN_a +H₂OMMIN_b +H₂O

Figure S1: Two different conformers of N,N-dimethylisopropylamine (MMIN) monomer (MMIN_a and MMIN_b) and its monohydrate (MMIN_a+H₂O and MMIN_b+H₂O). The global minimum structure is MMIN_a for the monomer and (less pronounced) MMIN_a+H₂O for the monohydrate.

Table S8: Relative electronic ΔE_{el} and zero point corrected ΔE_0 energy of two different monomers of N,N-dimethylcyclohexylamine (MMCN): MMCN_a and MMCN_b and two different heterodimer with water: MMCN_a+H₂O and MMCN_b+H₂O using B3LYP-D3/def2-TZVP. These conformer structures are shown in Fig. S2.

Conformer	$\Delta E_{el}/(\text{kJ/mol})$	$\Delta E_0/(\text{kJ/mol})$	Conformer	$\Delta E_{el}/(\text{kJ/mol})$	$\Delta E_0/(\text{kJ/mol})$
MMCN_a	0	0	MMIN_a+H ₂ O	0	0
MMCN_b	2.3	2.7	MMIN_b+H ₂ O	1.2	1.3

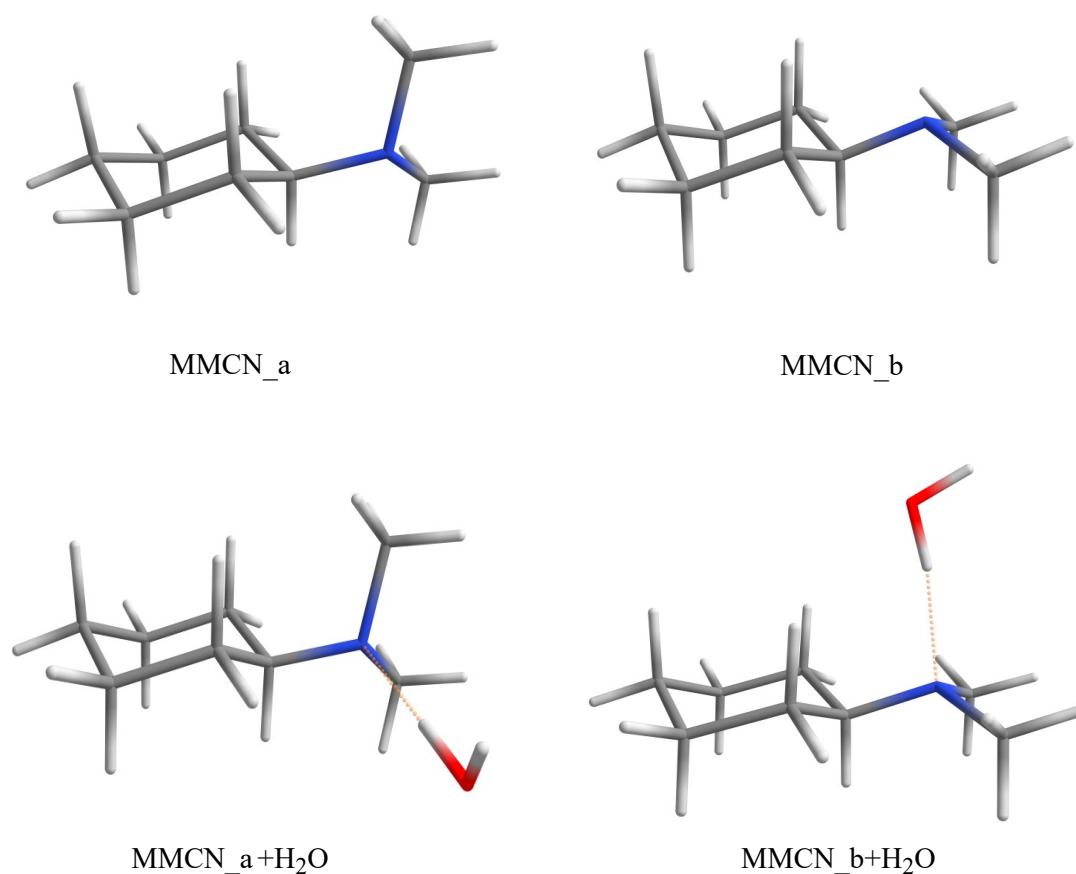


Figure S2: Two different conformers of N,N-dimethylcyclohexylamine (MMCN) monomer (MMCN_a and MMCN_b) and its monohydrate (MMCN_a+H₂O and MMCN_b+H₂O). The global minimum structure is MMCN_a for the monomer and (less pronounced) MMCN_a+H₂O for the monohydrate.

4 Four anharmonic coupling models

Four different coupling models A, B, C and C' are shown in Figs. S3, S4, S5 and S6 to explain anharmonic resonance scenarios for a bright OH stretching vibration OHb sharing its intensity with the bending overtone b2 and the combination bands b2ON, b2ON2 and OHbON in tertiary amines monohydrates. Shown are progressions of ON stretching levels building on OHb (left, black) and on b2 (right, red). The resulting coupling matrices (2×2 matrix for model A, 3×3 matrix for model B, 4×4 matrix for model C and C') are derived in ESI part 3. The obtained coupling constants W and the deperturbed positions of different resonance partners are listed in Table S9, S10, S11, S12.

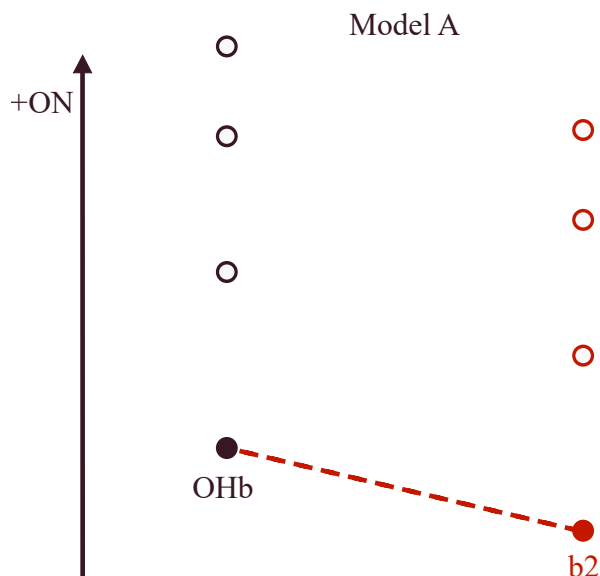


Figure S3: Coupling model A

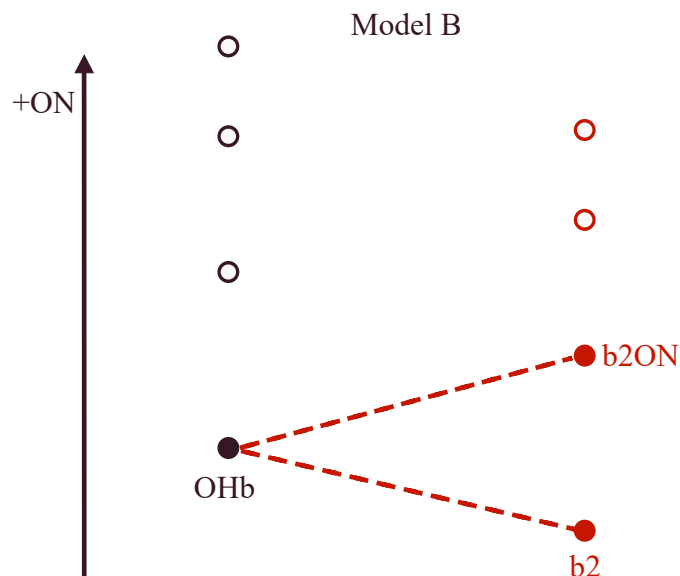


Figure S4: Coupling model B

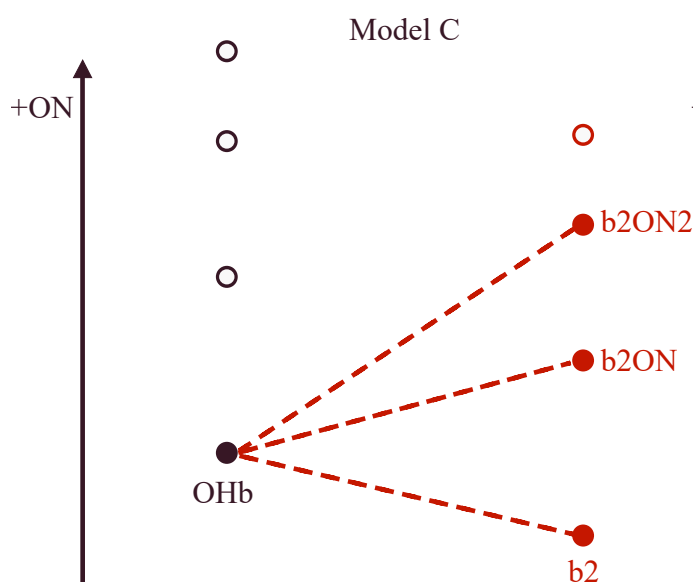


Figure S5: Coupling model C

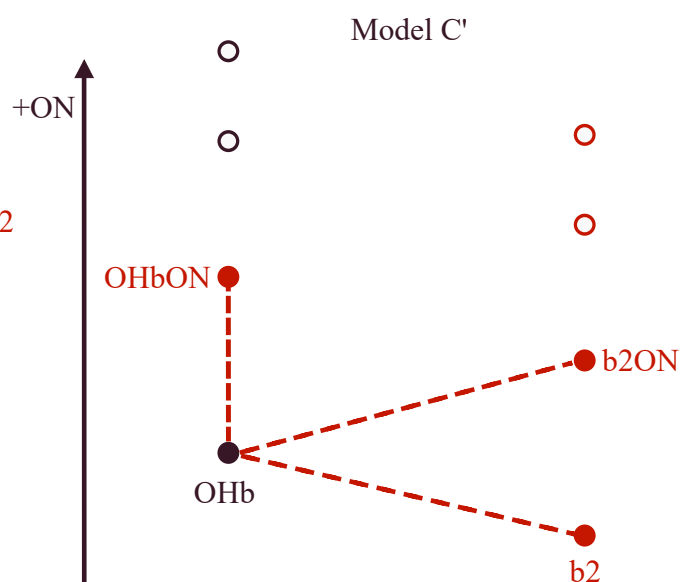


Figure S6: Coupling model C'

Table S9: Coupling constants W_2 with their uncertainties ΔW_2 and deperturbed positions for b2 and OHb with associated uncertainties $\Delta b2$ and ΔOHb derived from coupling model A

Code	b2	$\Delta b2$	OHb	ΔOHb	W_2	ΔW_2
MMEN	3217.48	3.54	3274.86	3.54	46.48	2.21
MN4	3217.53	4.39	3272.48	4.34	46.43	2.72
MMIN	3221.66	2.02	3250.03	2.03	46.72	0.66
MN5	3214.80	4.55	3263.30	4.51	43.80	2.71
MMTN	3219.89	2.46	3228.92	2.45	43.87	0.38
N555	3229.34	2.94	3260.62	2.96	49.19	0.99
MMCN	3220.42	3.68	3247.66	3.69	45.84	1.11
MN5MMMM	3217.79	2.72	3215.83	2.72	40.54	0.28

Table S10: Coupling constants W_2 , W_3 with their uncertainties ΔW_2 , ΔW_3 and deperturbed positions for b2, OHb and b2ON with associated uncertainties $\Delta b2$, ΔOHb and $\Delta b2ON$ derived from coupling model B

Code	b2	$\Delta b2$	OHb	ΔOHb	b2ON	$\Delta b2ON$	W_2	ΔW_2	W_3	ΔW_3
MMEN	3213.64	3.07	3291.31	3.17	3338.99	1.37	46.07	2.50	23.72	0.96
MN4	3214.04	4.02	3286.88	4.33	3336.68	1.39	46.13	3.06	21.99	1.05
MMIN	3218.84	1.86	3264.54	1.77	3336.33	0.85	48.00	0.86	27.67	0.88
MN5	3212.64	4.34	3273.80	4.70	3333.93	1.39	43.99	2.97	20.99	1.45
MMTN	3217.05	2.39	3247.43	3.50	3328.79	2.49	46.44	0.74	35.25	2.20
N555	3225.15	2.59	3277.62	2.61	3338.38	1.44	50.31	1.33	26.11	1.18
MMCN	3216.55	3.30	3267.74	3.64	3330.91	2.28	47.60	1.63	31.57	1.69
MN5MMMM	3214.92	2.68	3236.10	4.90	3316.81	4.21	43.86	0.88	37.37	3.52

Table S11: Deperturbed positions for b2, OHb, b2ON and xONn with associated uncertainties $\Delta b2$, ΔOHb , $\Delta b2ON$ and $\Delta xONn$ derived from coupling model C

Code	b2	$\Delta b2$	OHb	ΔOHb	b2ON	$\Delta b2ON$	xONn	$\Delta xONn$
MMEN	3213.46	3.05	3294.29	3.76	3338.88	1.38	3443.75	2.79
MN4	3213.72	3.99	3292.00	5.07	3336.52	1.40	3436.74	2.60
MMIN	3218.44	1.84	3270.31	3.15	3336.03	0.89	3425.52	2.74
MN5	3212.18	4.29	3281.48	5.28	3333.68	1.42	3422.52	2.50
MMTN	3216.70	2.38	3252.45	4.12	3328.31	2.53	3409.02	2.46
N555	3224.68	2.55	3283.99	3.73	3338.10	1.46	3434.94	3.00
MMCN	3216.15	3.26	3273.45	3.76	3330.52	2.31	3421.73	1.45
MN5MMMM	3214.02	2.64	3248.25	4.69	3315.20	4.30	3383.47	2.04

Table S12: Coupling constants W_2 , W_3 and W_4 and their uncertainties ΔW_2 , ΔW_3 and ΔW_4 derived from coupling model C

Code	W_2	ΔW_2	W_3	ΔW_3	W_4	ΔW_4
MMEN	46.22	2.53	24.07	1.01	17.14	8.55
MN4	46.40	3.11	22.58	1.09	23.66	7.74
MMIN	48.48	0.93	28.69	1.05	25.58	7.17
MN5	44.45	3.06	22.03	1.49	30.12	4.58
MMTN	46.98	0.81	36.52	2.26	22.61	6.76
N555	50.82	1.41	27.01	1.27	26.71	7.08
MMCN	48.07	1.70	32.62	1.72	25.13	3.34
MN5MMMM	45.37	0.94	41.09	3.38	32.60	3.45

5 Isotope effect in the monohydrates of tertiary amines

When normal water HOH is replaced by singly deuterated water DOH, there is only one signal for the hydrogen-bonded OH stretching fundamental in the monohydrate because the resonance partners are removed. To estimate the deperturbed position of OHb in the 1:1 complex of tertiary amine with normal water HOH, the calculated harmonic wavenumber difference between HOH and DOH is subtracted from the experimental OH stretching vibration in the heterodimer with DOH, as shown in Figs. 1 and 2 from the main text and Fig. S7, S8, S9 and S10. The experimental and harmonic wavenumbers are listed in Table S13 and S14.

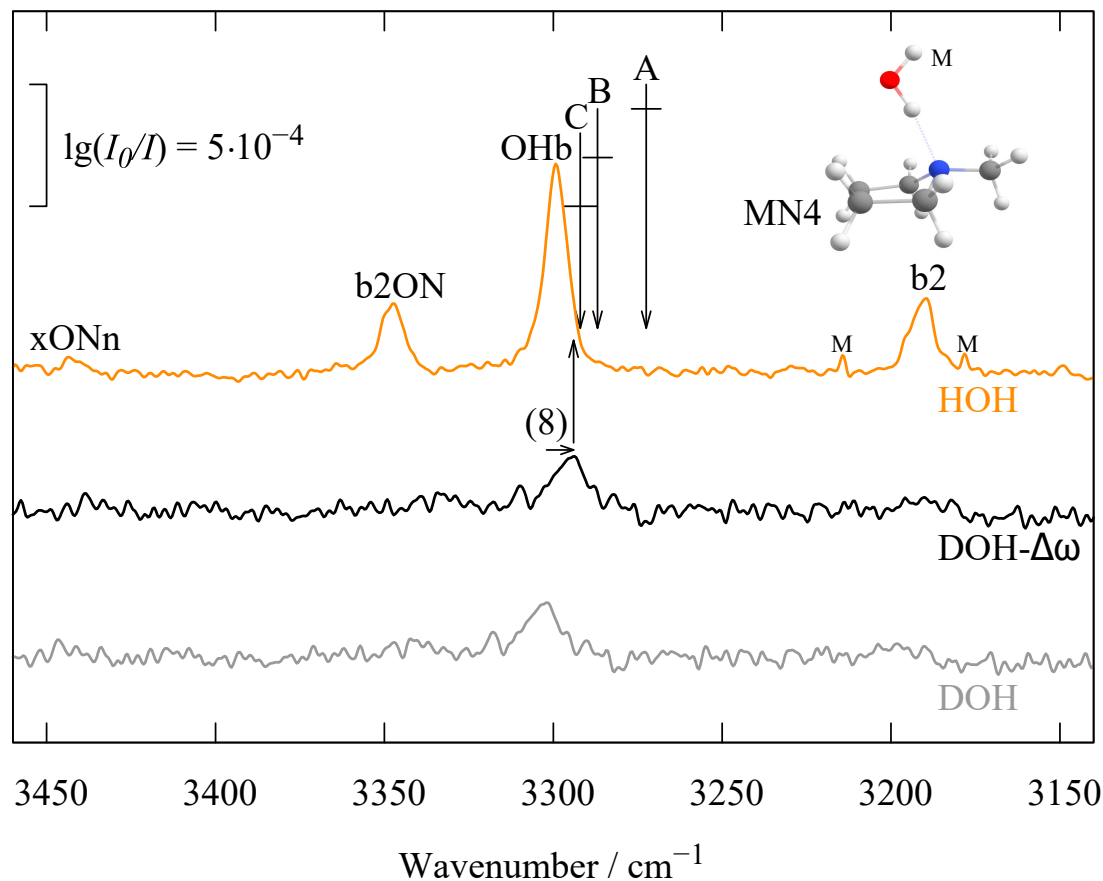


Figure S7: Analogous to Fig. 1 and 2 from the main text. The good agreement of the 4-transition intensity centroid of the OH stretching spectrum of the N-methylpyrrolidine- H_2O complex (upper trace, arrow C) with the OH stretching spectrum of the corresponding HOD complex (lower trace) after harmonic correction for kinematic effects ($\Delta\omega = 8 \text{ cm}^{-1}$, middle trace) suggests that all four 1:1 complex transitions in the upper trace are likely to derive their intensity from the OH stretching mode. Arrows mark centroid positions and are labelled according to models A, B, C.

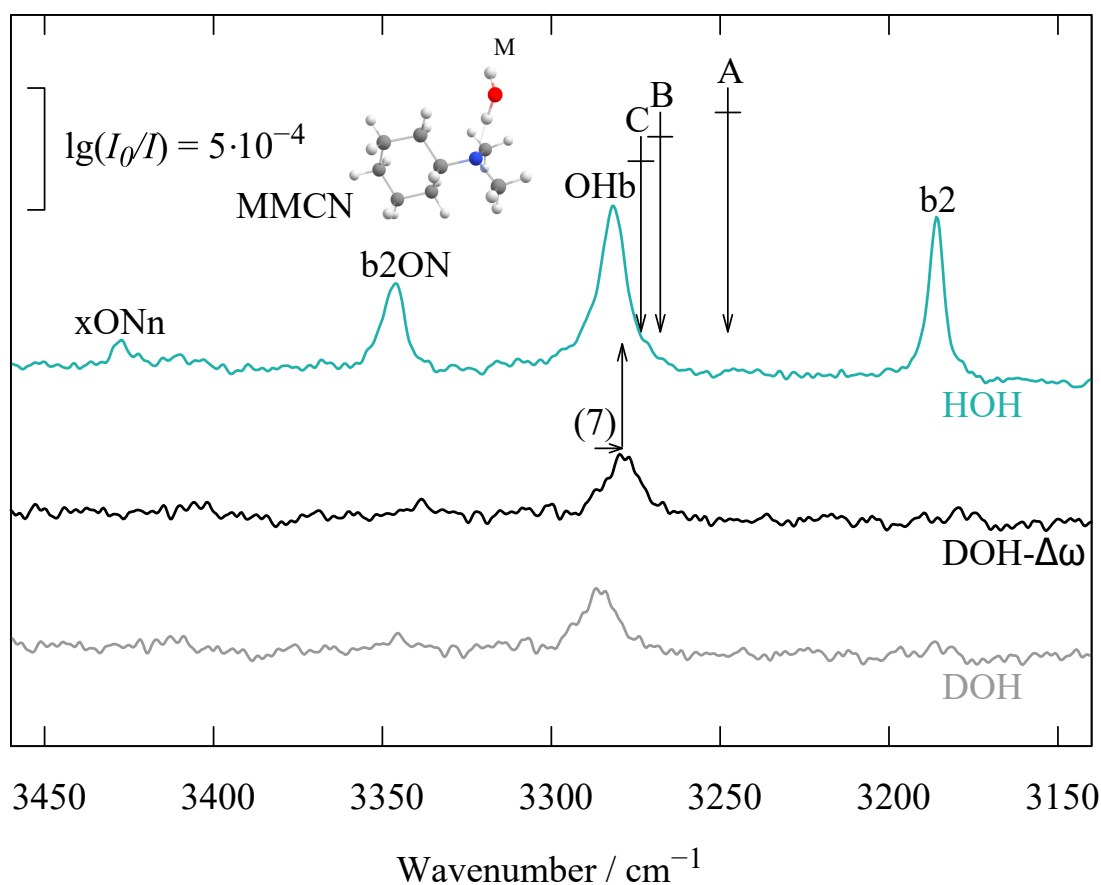


Figure S8: Analogous to Fig. 1 and 2 from the main text. The good agreement of the 4-transition intensity centroid of the OH stretching spectrum of the N,N-dimethylcyclohexylamine-H₂O complex (upper trace, arrow C) with the OH stretching spectrum of the corresponding HOD complex (lower trace) after harmonic correction for kinematic effects ($\Delta\omega = 7 \text{ cm}^{-1}$, middle trace) suggests that all four 1:1 complex transitions in the upper trace are likely to derive their intensity from the OH stretching mode. Arrows mark centroid positions and are labelled according to models A, B, C.

Table S13: Experimental wavenumbers $\tilde{\nu}$ of OHb for tertiary amines with DOH and the harmonic wavenumbers ω and the harmonic wavenumber differences $\Delta\omega$ between DOH and HOH for five tertiary amines: MN4, MN5, MMCN, MMTN and MN5MMMM. The experimental deperturbed position of OHb for HOH is calculated by subtracting the harmonic wavenumber difference $\Delta\omega$ from the experimental wavenumber $\tilde{\nu}(\text{DOH})$. See Figs. 1 and 2 from the main text and Figs. S7, S8 and S9 from ESI.

Code	$\tilde{\nu}/\text{cm}^{-1}$	ω/cm^{-1}		$\Delta\omega$	$\tilde{\nu}(\text{DOH})-\Delta\omega$
	DOH	HOH	DOH		
MN4	3302	3384	3392	8	3294
MN5	3294	3370	3378	8	3286
MMCN	3286	3366	3373	7	3279
MMTN	3269	3342	3351	9	3260
MN5MMMM	3256	3333	3341	8	3248

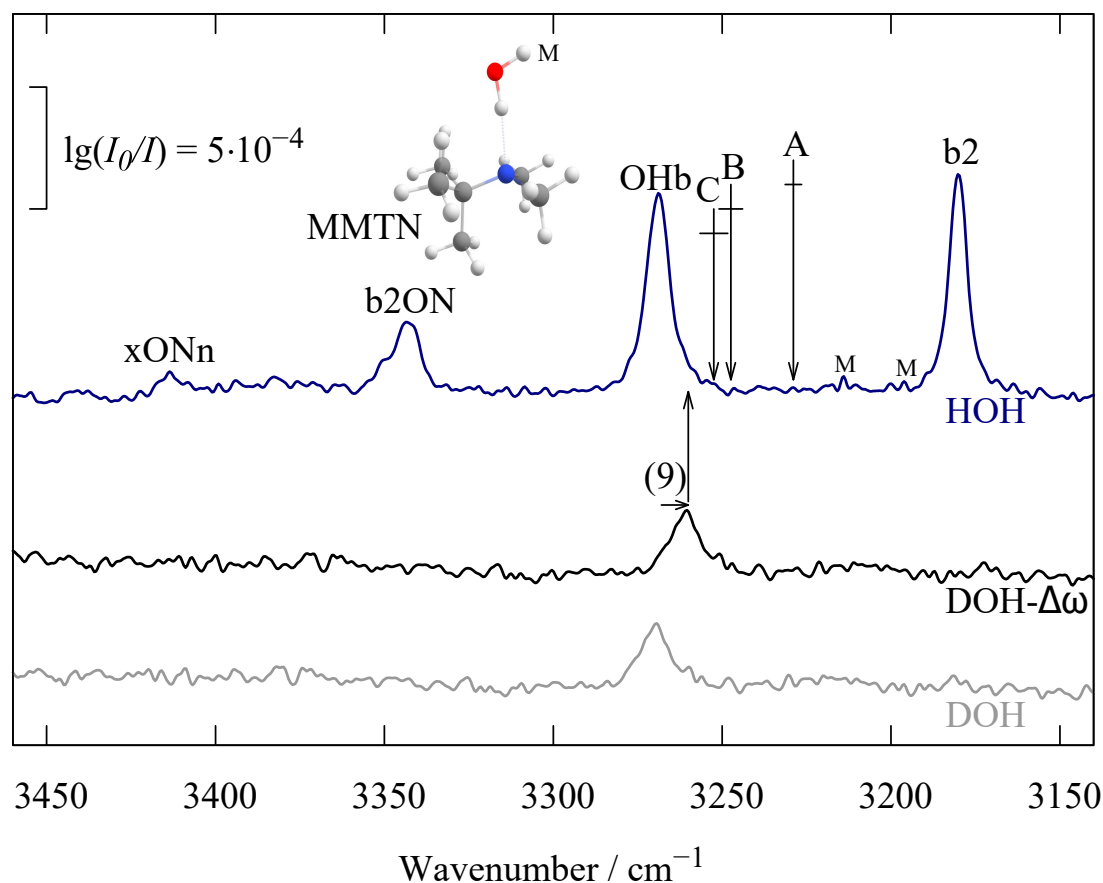


Figure S9: Analogous to Fig. 1 and 2 from the main text. The good agreement of the 4-transition intensity centroid of the OH stretching spectrum of the *tert*-butyldimethylamine-H₂O complex (upper trace, arrow C) with the OH stretching spectrum of the corresponding HOD complex (lower trace) after harmonic correction for kinematic effects ($\Delta\omega = 9\text{ cm}^{-1}$, middle trace) suggests that all four 1:1 complex transitions in the upper trace are likely to derive their intensity from the OH stretching mode. Arrows mark centroid positions and are labelled according to models A, B, C.

Table S14: Raw and deperturbed wavenumbers (in cm^{-1}) of OHb stretching fundamental for the heterodimers of five tertiary amines: MN4, MN5, MMCN, MMTN and MN5MMMM. The raw experimental wavenumbers $\tilde{\nu}(\text{raw})$ with HOH and DOH are listed. The deperturbed positions of OHb centroid A, centroid B and centroid C are calculated by using coupling models A, B, C which are shown in detail in Tables S9, S10 and S11. The experimental deperturbed position for HOH, which is calculated by subtracting the harmonic wavenumber difference $\Delta\omega$ between DOH and HOH from the experimental wavenumber $\tilde{\nu}(\text{DOH})$, is shown to compare with centroid A, B and C, and also calculated the difference from centroid C in the last column. See Fig. 3 from the main document.

Code	HOH			DOH	$\tilde{\nu}(\text{DOH})-\Delta\omega$	$(\tilde{\nu}(\text{DOH})-\Delta\omega)$ -centroid C	
	$\tilde{\nu}(\text{raw})$	centroid A	centroid B	centroid C			
MN4	3299	3273	3287	3292	3302	3294	2
MN5	3289	3264	3274	3282	3294	3286	5
MMCN	3282	3248	3268	3273	3286	3279	6
MMTN	3269	3235	3247	3252	3269	3260	8
MN5MMMM	3257	3219	3236	3248	3256	3248	0

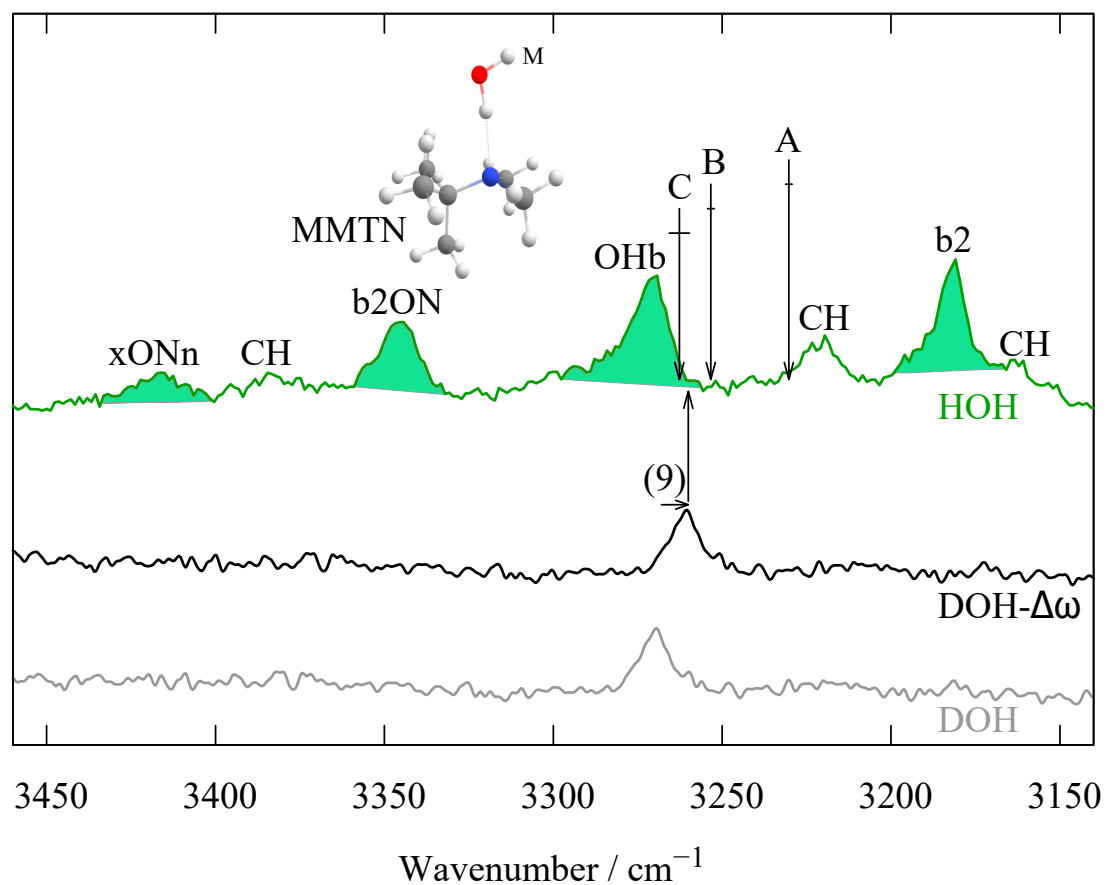


Figure S10: Same as Fig. S9, but with the FTIR spectrum replaced by the Raman spectrum of MMTN with HOH, also showing the same good agreement for arrow C with the OH stretching spectrum of the corresponding HOD complex. Arrows mark centroid positions and are labelled according to models A, B, C. The arrow positions are 3230 cm^{-1} for model A, 3253 cm^{-1} for B and 3263 cm^{-1} for C. The shaded areas in the upper Raman spectrum are used to calculate the centroid C.

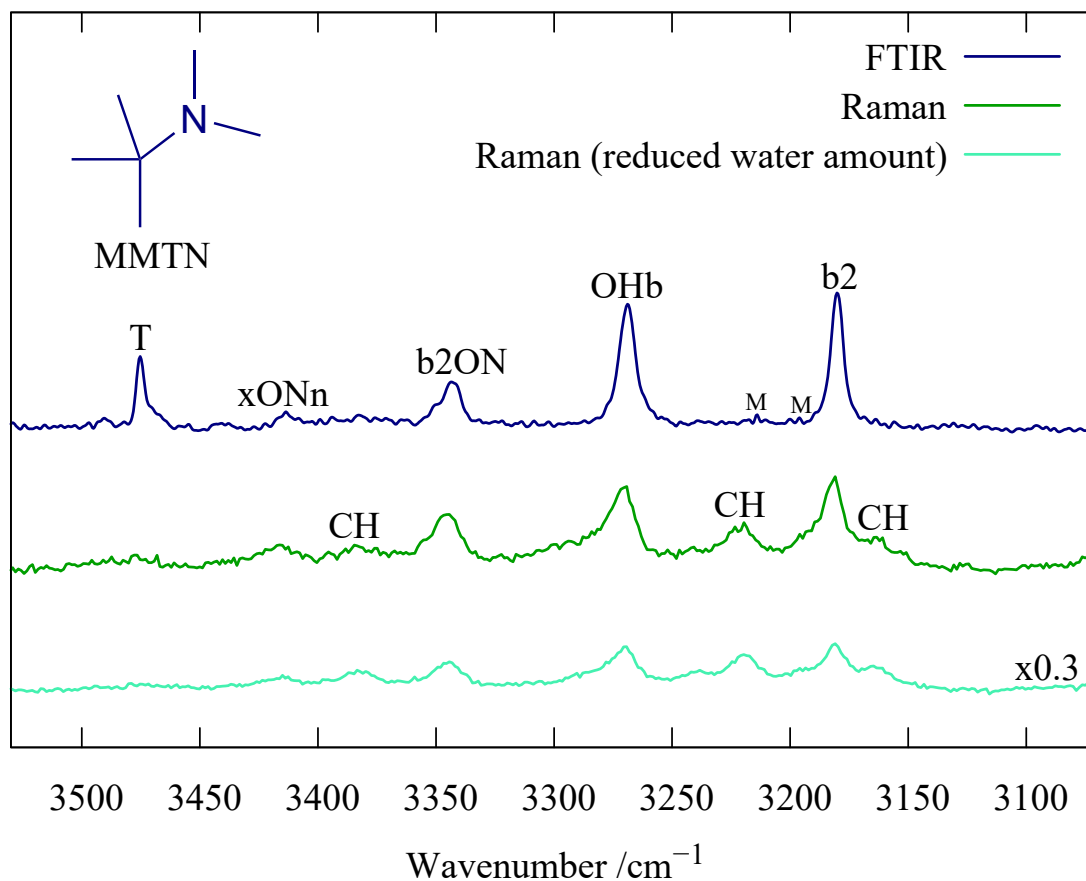


Figure S11: Analogous to Fig. 4 from the main text. Demonstration of wave function mixing of the OHb state in the MMTN monohydrate by observing largely the same relative intensity pattern in IR (top) and Raman (middle) spectroscopy, apart from CH combination bands in the Raman spectrum which persist for reduced water amount (bottom trace, multiplied by 0.3 because the amine concentration was higher).

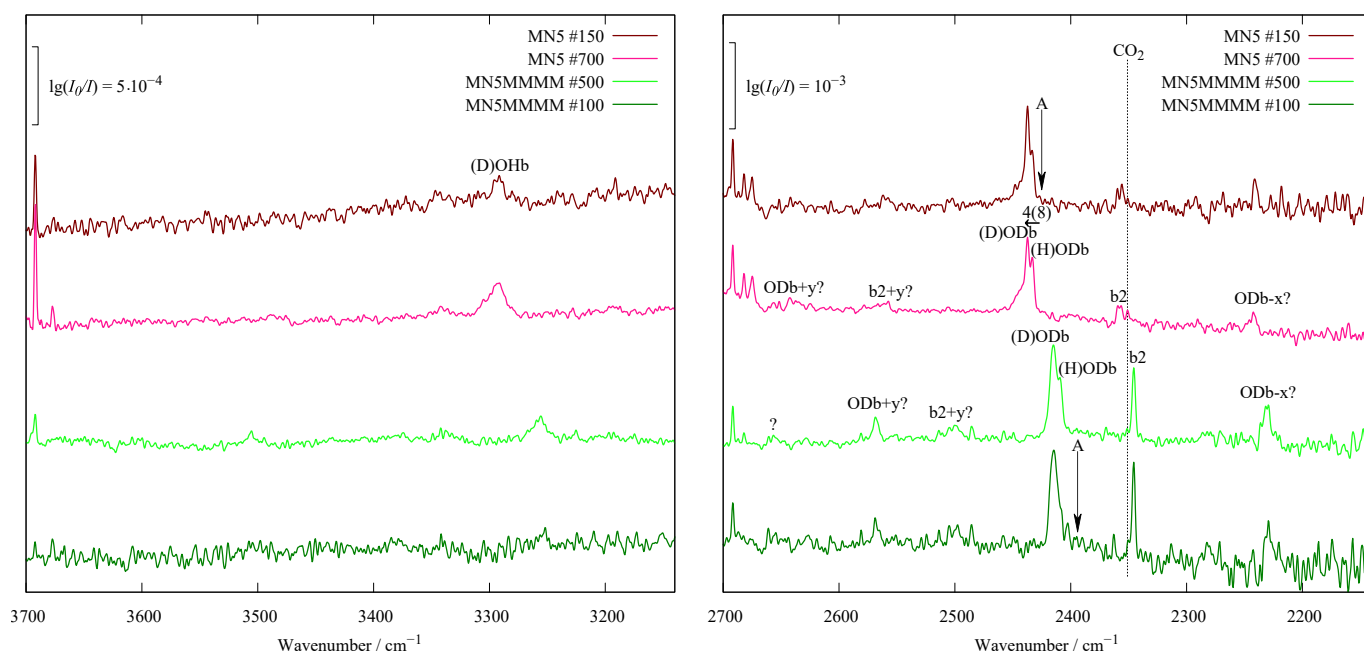


Figure S12: The spectra for isotope substitution of water with 1-methylpiperidine (MN5) and 1,2,2,6,6-pentamethylpiperidine (MN5MMMM). The concentration of D_2O is dropping in favour of less D-rich isotopologs. In the early 150 scans of MN5 (top spectrum) and the early 100 scans of MN5MMMM (bottom spectrum), D_2O dominates and a significant (D)ODb peak can be seen clearly. In the later 700 scans of MN5 and 500 scans of MN5MMMM (central spectra), the concentrations of DOH and HOD are increasing, as evidenced by (D)OHb and the (D)ODb/(H)ODb doublet. The black arrow A is the deperturbed position of (D)ODb from the Fermi resonance analysis of (D)ODb with b2. Combination bands of ODb and b2 with dimer stretching or methyl torsion (predicted around $150\text{-}250\text{ cm}^{-1}$) may explain some of the weak features in the OD stretching range (right panel).

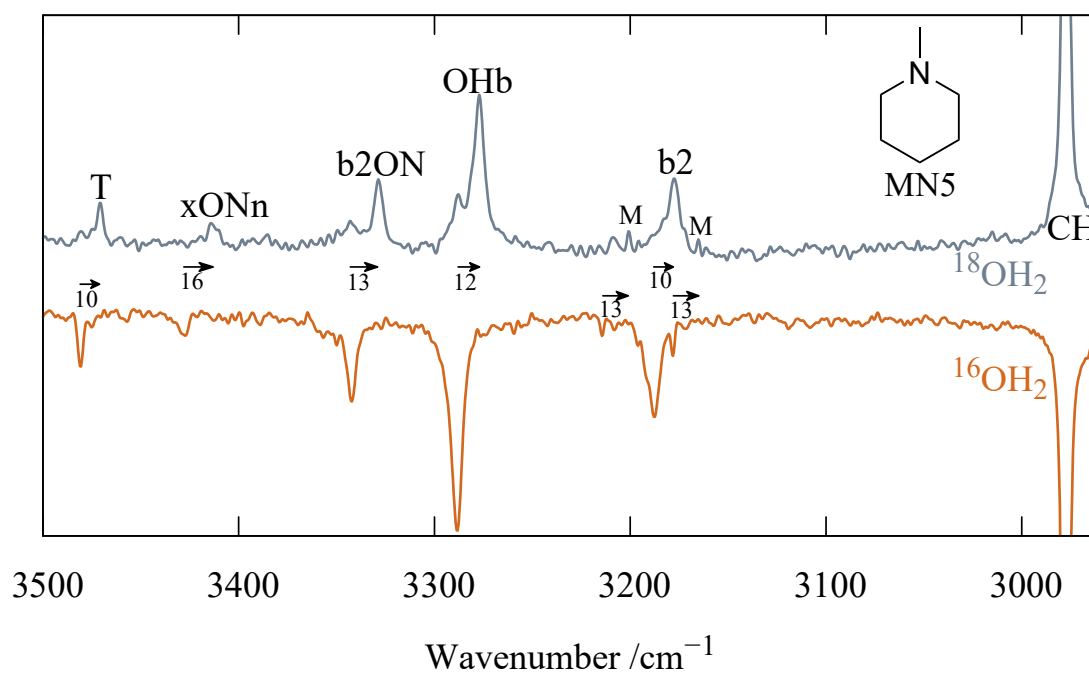


Figure S13: Same as Fig. 5 from the main document. Comparison of the OH stretching spectrum of MN5 with $^{16}OH_2$ (bottom, inverted) to the same spectrum enriched in $^{18}OH_2$. The 16-18-isotope shifts in cm^{-1} are clarified by arrows.

Table S15: Experimental wavenumbers $\tilde{\nu}$ of b2, OHb, b2ON and xONn for 1:1 complex of tertiary amines with $^{16}\text{OH}_2$ and $^{18}\text{OH}_2$ and M for water monomer and T for dihydrate. The downshift $\Delta\tilde{\nu}$ for the isotope effect between ^{16}O and ^{18}O is calculated. See Fig. 5 in the main text and Fig. S13 in ESI.

Code	$\tilde{\nu}/\text{cm}^{-1}$		$\Delta\tilde{\nu}/\text{cm}^{-1}$
	$^{16}\text{OH}_2$	$^{18}\text{OH}_2$	
N555			
b2	3193	3183	10
OHb	3297	3286	11
b2ON	3351	3336	15
xONn	3441	3424	17
T	3475	3465	10
M1	3214	3201	13
M2	3178	3165	13
MN5			
b2	3189	3179	10
OHb	3289	3277	12
b2ON	3342	3329	13
xONn	3429	3413	16
T	3481	3471	10
M1	3214	3201	13
M2	3178	3165	13

6 Perturbed and deperturbed ON stretching vibration in models C and C'

Table S16: Raw and deperturbed wavenumbers (in cm^{-1}) by applying model C for ON stretching vibration and its overtone 2ON of 8 tertiary amines: MMEN, MN4, MMIN, MN5, MMTN, N555, MMCN and MN5MMMM with water. The ON stretching fundamental is obtained by b2ON-b2 and its overtone 2ON is calculated as b2ON2(xONn)-b2 with their uncertainties ΔON and $\Delta 2\text{ON}$. The mass of amines in atomic mass units u is also shown. See Fig. 7 in the main text.

Code	Mass/ u	$\tilde{\nu}(\text{raw})$				Deperturbed by model C			
		ON(b2ON-b2)	ΔON	2ON(b2ON2-b2)	$\Delta 2\text{ON}$	ON(b2ON-b2)	ΔON	2ON(b2ON2-b2)	$\Delta 2\text{ON}$
MMEN	73	160.2	0.9	255.1	2.4	125.4	4.5	230.3	5.9
MN4	85	156.8	1.3	250.6	1.9	122.8	5.4	223.0	6.6
MMIN	87	161.0	0.6	243.6	1.7	117.6	2.8	207.1	4.6
MN5	99	153.6	1.4	240.8	2.4	121.5	5.8	210.3	6.8
MMTN	101	164.2	1.0	233.0	1.7	111.6	4.9	192.3	4.9
N555	111	157.9	0.9	247.3	2.0	113.4	4.1	210.2	5.6
MMCN	127	161.1	0.9	240.6	1.0	114.4	5.6	205.6	4.8
MN5MMMM	155	158.0	2.5	216.9	1.1	101.2	6.9	169.5	4.7

Table S17: Deperturbed wavenumbers (in cm^{-1}) by applying model C for ON stretching fundamental ν_1 and its overtone (2ON) $2\nu_1$ for 8 tertiary amines: MMEN, MN4, MMIN, MN5, MMTN, N555, MMCN and MN5MMMM with water. The anharmonicity constants $\omega_e x_e$ and ω_e are calculated by assuming a Morse oscillator. All values in cm^{-1} .

Code	ν_1	$2\nu_1$	$\omega_e x_e$	ω_e
MMEN	125.4	230.3	10.3	145.9
MN4	122.8	223.0	11.3	145.4
MMIN	117.6	207.1	14.1	145.8
MN5	121.5	210.3	16.3	154.2
MMTN	111.6	192.3	15.5	142.5
N555	113.4	210.2	8.3	130.0
MMCN	114.4	205.6	11.6	137.6
MN5MMMM	101.2	169.5	16.4	134.1

Table S18: Raw and deperturbed wavenumbers (in cm^{-1}) by applying model C' for ON stretching vibration on top of the b2 excitation and ON on top of OHb excitation for 8 tertiary amines: MMEN, MN4, MMIN, MN5, MMTN, N555, MMCN and MN5MMMM with water. The ON stretching fundamental on top of b2 is obtained by b2ON-b2 and ON on top of OHb is calculated as OHbON(xONn)-OHb with their uncertainties ΔON . The mass of amines by atomic unit u is also shown. See Fig. 8 from the main text.

Code	Mass/ u	$\tilde{\nu}(\text{raw})$				Deperturbed by model C'			
		ON(b2ON-b2)	ΔON	ON(OHbON-OHb)	ΔON	ON(b2ON-b2)	ΔON	ON(OHbON-OHb)	ΔON
MMEN	73	160.2	0.9	145.5	2.3	125.4	4.5	149.5	6.6
MN4	85	156.8	1.3	142.2	1.3	122.8	5.4	144.7	7.7
MMIN	87	161.0	0.6	145.9	1.8	117.6	2.8	155.2	5.9
MN5	99	153.6	1.4	140.1	1.9	121.5	5.8	141.0	7.8
MMTN	101	164.2	1.0	144.6	1.9	111.6	4.9	156.6	6.6
N555	111	157.9	0.9	143.9	2.3	113.4	4.1	150.9	6.8
MMCN	127	161.1	0.9	144.6	1.0	114.4	5.6	148.3	5.3
MN5MMMM	155	158.0	2.5	135.6	1.2	101.2	6.9	135.3	6.8

7 Quantum chemical bridging

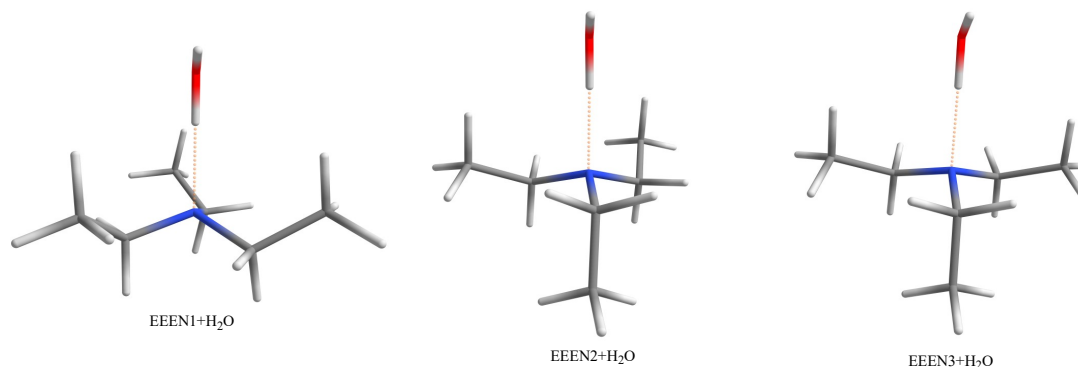


Figure S14: Three conformers of triethylamine (EEEN) heterodimer with water: EEEN1+H₂O, EEEN2+H₂O and EEEN3+H₂O. The global minimum structure is EEEN1+H₂O.

Table S19: Relative electronic ΔE_{el} and zero point corrected ΔE_0 energy of three different conformers of triethylamine (EEEN): EEEN1, EEEN2 and EEEN3 using B3LYP-D3/def2-TZVP. The energy barriers between conformers are also shown both in relative electronic ΔE_{el} and zero point corrected ΔE_0 energy. All of the relative energies are calculated from the energy of the global minimum conformer. These conformer structures are shown in Fig. 9 from the main text.

Conformer	$\Delta E_{el}/(\text{kJ/mol})$	$\Delta E_0/(\text{kJ/mol})$	Barrier	$\Delta E_{el}/(\text{kJ/mol})$	$\Delta E_0/(\text{kJ/mol})$
EEEN1	0	0	EEEN3 to EEEN1	26.1	25.9
EEEN2	2.3	3	EEEN2 to EEEN1	23.8	23.7
EEEN3	2.1	3.2	EEEN3 to EEEN2	8.7	8.5

Table S20: Relative electronic ΔE_{el} and zero point corrected ΔE_0 energy and the harmonic wavenumber ω/cm^{-1} of b2, OHb, b2ON, b2ON2 and OHbON for three different conformers of triethylamine (EEEN) with water: EEEN1+H₂O, EEEN2+H₂O and EEEN3+H₂O using B3LYP-D3/def2-TZVP. These conformer structures are shown in Fig. S14.

Conformer	$\Delta E_{el}/(\text{kJ/mol})$	$\Delta E_0/(\text{kJ/mol})$	b2	OHb	b2ON	b2ON2	OHbON
EEEN1+H ₂ O	0	0	3320.1	3376.7	3476.7	3633.2	3533.3
EEEN2+H ₂ O	1.8	1.9	3329.8	3350.7	3488.9	3648.0	3509.8
EEEN3+H ₂ O	0.9	1.2	3326.4	3345.9	3489.4	3652.5	3508.9

Table S21: Harmonic and deperturbed wavenumbers (in cm^{-1}) of b2, OHb, b2ON and b2ON2 for three different conformers of EEEN monohydrates: EEEN1, EEEN2 and EEEN3 by applying the coupling model C.

Code	ω by model C				correction by model C				Deperturbed $\tilde{\nu}$ by model C			
	b2	OHb	b2ON	b2ON2	b2	OHb	b2ON	b2ON2	b2	OHb	b2ON	b2ON2
EEEN1+H2O	3320	3377	3477	3633	103	89	150	223	3217	3288	3327	3410
EEEN2+H2O	3330	3351	3489	3648	103	89	150	223	3227	3262	3339	3425
EEEN3+H2O	3326	3346	3489	3653	103	89	150	223	3223	3257	3339	3430

Table S22: Perturbed wavenumbers $\tilde{\nu}$ (in cm^{-1}) for b2, OHb, b2ON and b2ON2 and their perturbed intensities I for three different conformers of EEEN monohydrates: EEEN1, EEEN2 and EEEN3 by applying the coupling model C. See Fig. 10 from the main text.

Code	Perturbed $\tilde{\nu}$ by model C				Perturbed I by model C			
	b2	OHb	b2ON	b2ON2	b2	OHb	b2ON	b2ON2
EEEN1+H2O	3192	3290	3344	3416	0.22	0.48	0.25	0.05
EEEN2+H2O	3191	3282	3350	3429	0.36	0.50	0.12	0.03
EEEN3+H2O	3187	3279	3350	3433	0.36	0.51	0.11	0.02

Table S23: Harmonic and deperturbed wavenumbers (in cm^{-1}) of b2, OHb, b2ON and OHbON for three different conformers of EEEN monohydrates: EEEN1, EEEN2 and EEEN3 by applying the coupling model C'.

Code	ω by model C'				correction by model C'				Deperturbed $\tilde{\nu}$ by model C'			
	b2	OHb	b2ON	OHbON	b2	OHb	b2ON	OHbON	b2	OHb	b2ON	OHbON
EEEN1+H2O	3320	3377	3477	3533	103	89	150	105	3217	3288	3327	3428
EEEN2+H2O	3330	3351	3489	3510	103	89	150	105	3227	3262	3339	3405
EEEN3+H2O	3326	3346	3489	3509	103	89	150	105	3223	3257	3339	3404

Table S24: Perturbed wavenumbers $\tilde{\nu}$ (in cm^{-1}) for b2, OHb, b2ON and OHbON and their perturbed intensities I for three different conformers of EEEN monohydrates: EEEN1, EEEN2 and EEEN3 by applying the coupling model C'. See Fig. 10 from the main text.

Code	Perturbed $\tilde{\nu}$ by model C'				Perturbed I by model C'			
	b2	OHb	b2ON	OHbON	b2	OHb	b2ON	OHbON
EEEN1+H2O	3192	3290	3345	3433	0.22	0.48	0.26	0.04
EEEN2+H2O	3191	3282	3349	3410	0.36	0.49	0.11	0.04
EEEN3+H2O	3187	3278	3349	3409	0.36	0.50	0.10	0.04

8 Methylation instead of deuteration

Table S25: Harmonic wavenumber ω for two vibrations ON_1 and ON_2 with ON stretching character and OH stretching fundamental OHb of the heterodimer of tertiary amines with methanol and experimental wavenumber $\tilde{\nu}$ for OHb. See Fig. 11 from the main document.

Code	ω/cm^{-1}			$\tilde{\nu}/\text{cm}^{-1}$
	ON_1	ON_2	OHb	OHb
MN4	178.5	121.3	3381.7	3287
MMCN	181.6	125.8	3359.4	3262
MMTN	187.0	121.4	3342.6	3249
MN5MMMM	185.9	116.0	3329.1	3226

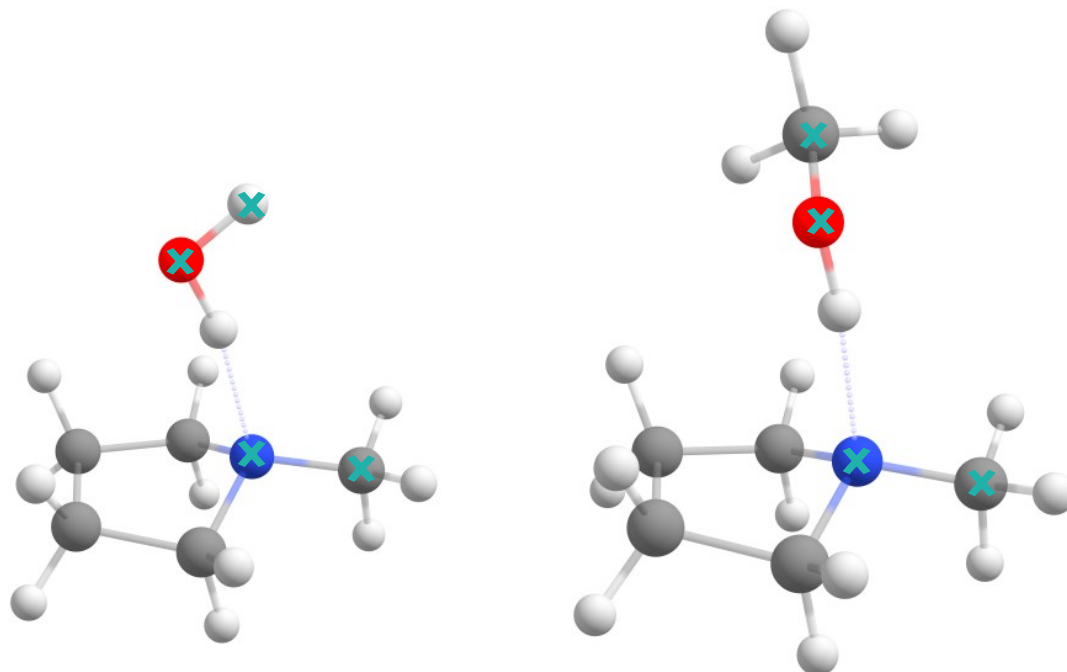


Figure S15: Torsion angle around hydrogen bond $\angle\text{CNOH}$ for the exemplary monohydrate of tertiary amines with water and $\angle\text{CNOC}$ with methanol. The atoms included in the torsion angle are labelled "X". The angles are described in Table S26.

Table S26: Torsion angles around hydrogen bond $\angle\text{CNOH}$ for the monohydrate of tertiary amines with water and $\angle\text{CNOC}$ with methanol using B3LYP-D3/def2-TZVP.

Code	H ₂ O $\angle\text{CNOH}$	MeOH $\angle\text{CNOC}$
MN4	2	84
MMCN	106	56
MMTN	175	115
MN5MMMM	0	0

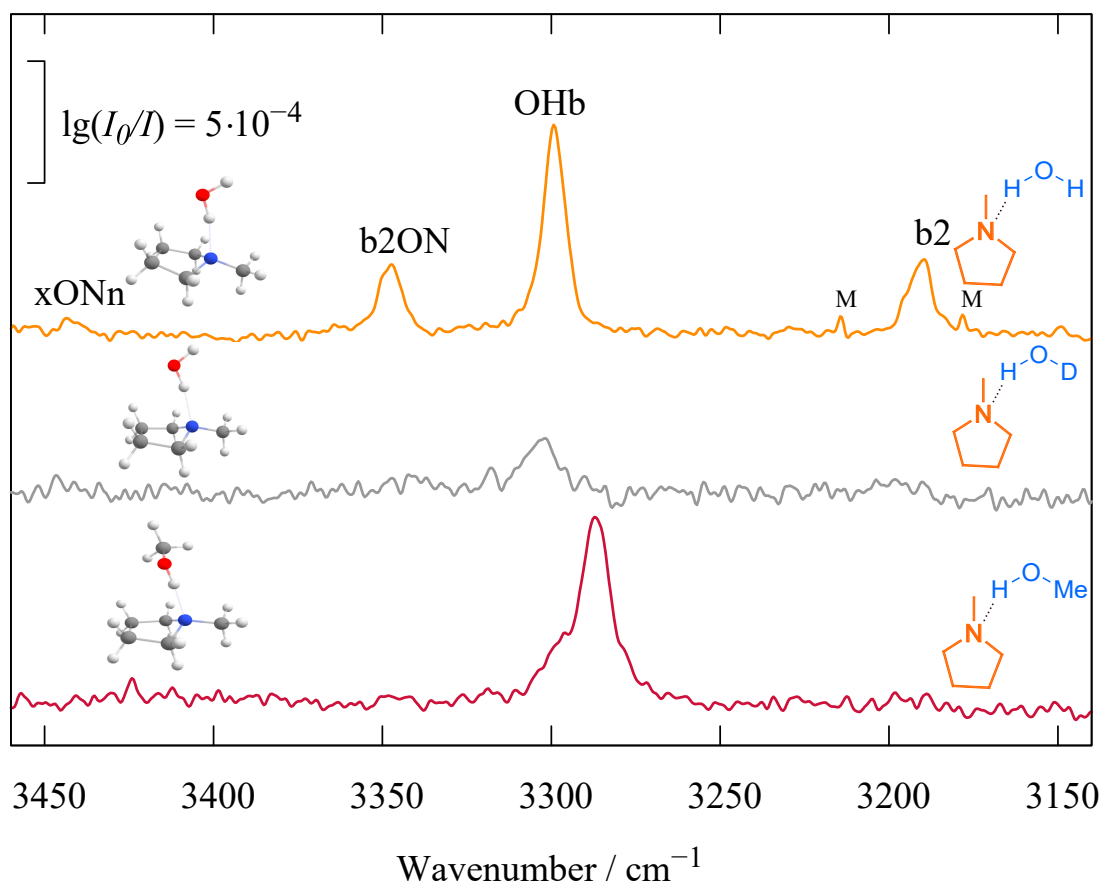


Figure S16: Spectra for the monohydrate of N-Methylpyrrolidine with HOH, DOH and MeOH. The upper trace is the monohydrate of N-Methylpyrrolidine with HOH which have four signals: OHb, b2, b2ON and xONn through anharmonic resonance. The middle trace is for the monohydrate with DOH and the lower one is with methanol. Both of them have a single OHb signal.

9 Dihydrate contributions to the HyDRA database

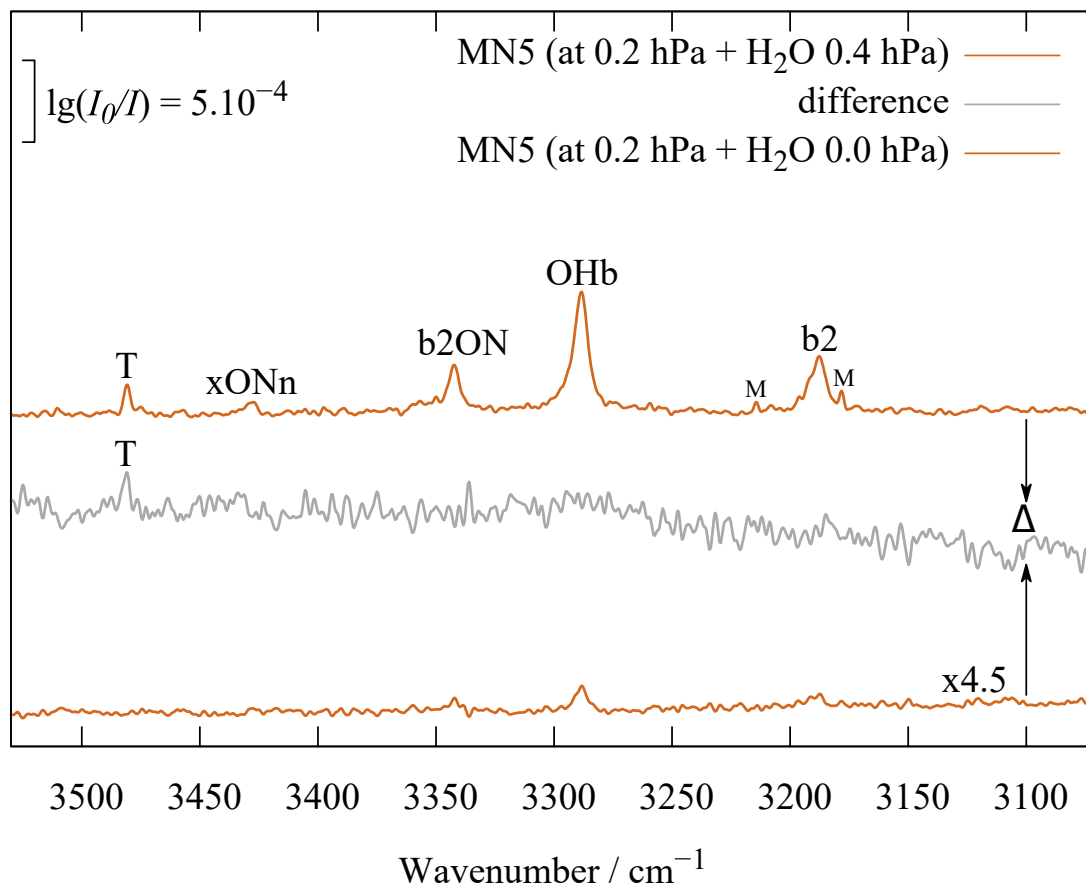


Figure S17: The dihydrate WWA for MN5 can be clearly separated from the heterodimer features. T is the raw dihydrate signal for indirect solvation contact.

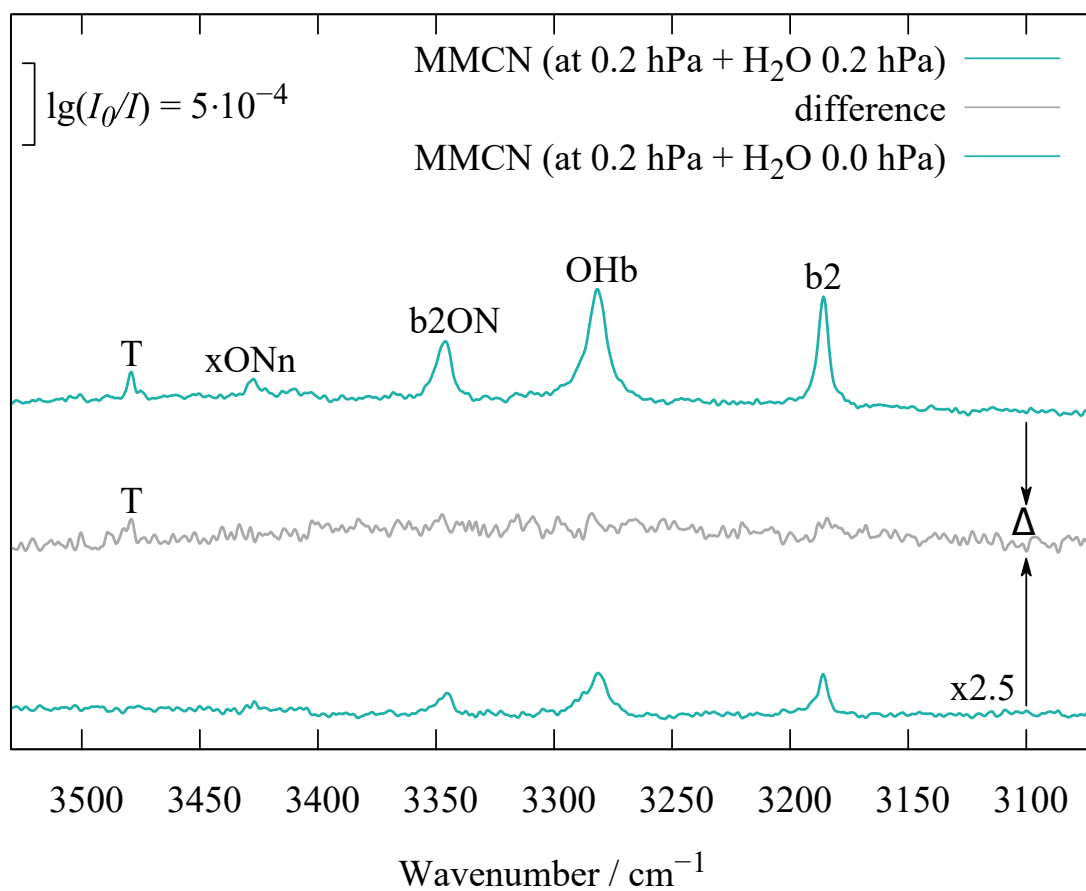


Figure S18: The dihydrate WWA for MMCN can be clearly separated from the heterodimer features. T is the raw dihydrate signal for indirect solvation contact.

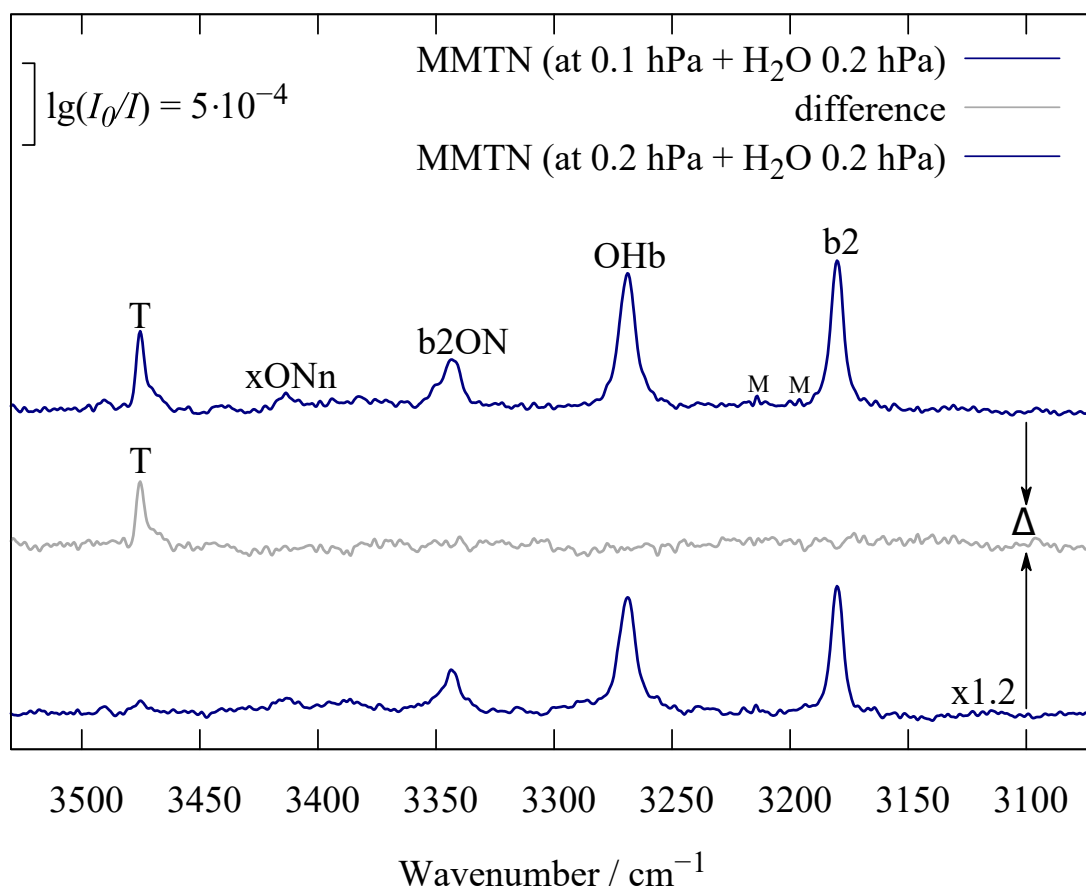


Figure S19: The dihydrate WWA for MMTN can be clearly separated from the heterodimer features. T is the raw dihydrate signal for indirect solvation contact.

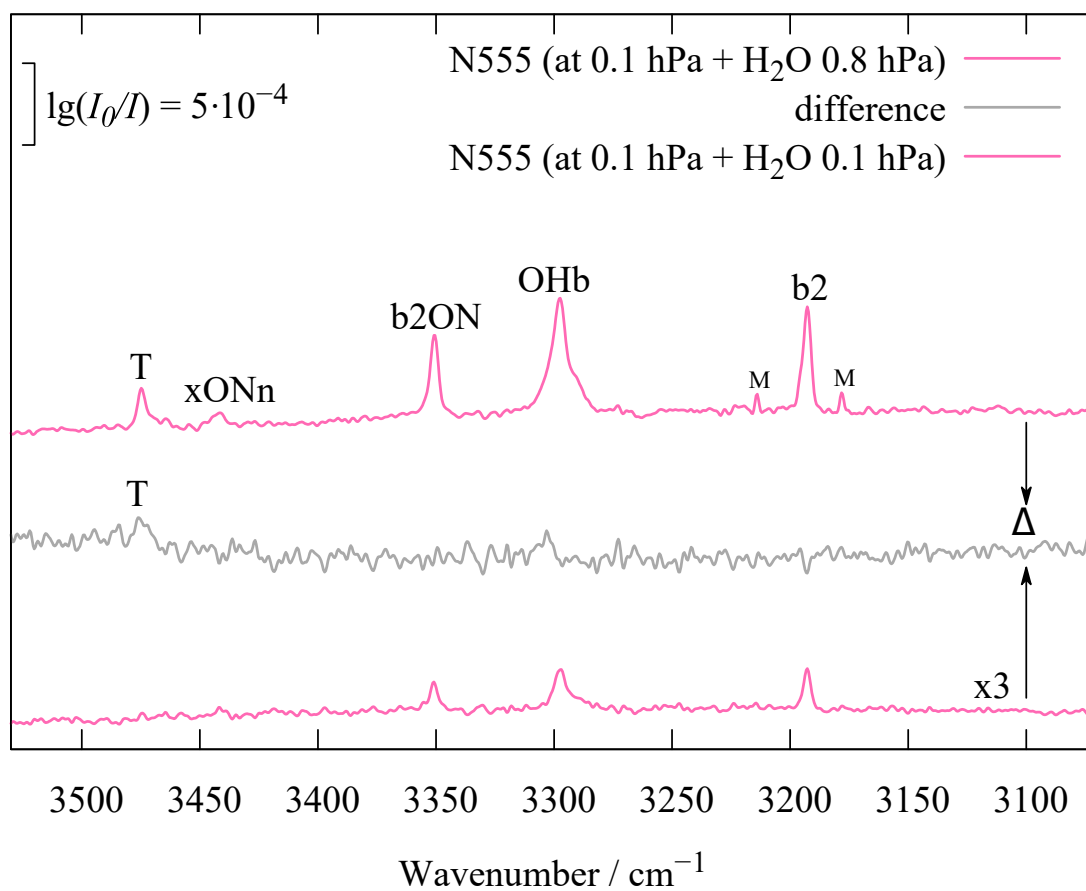


Figure S20: The dihydrate WWA for N555 can be clearly separated from the heterodimer features. T is the raw dihydrate signal for indirect solvation contact.

10 Experimental spectra of triisopropylamine (IIIN)

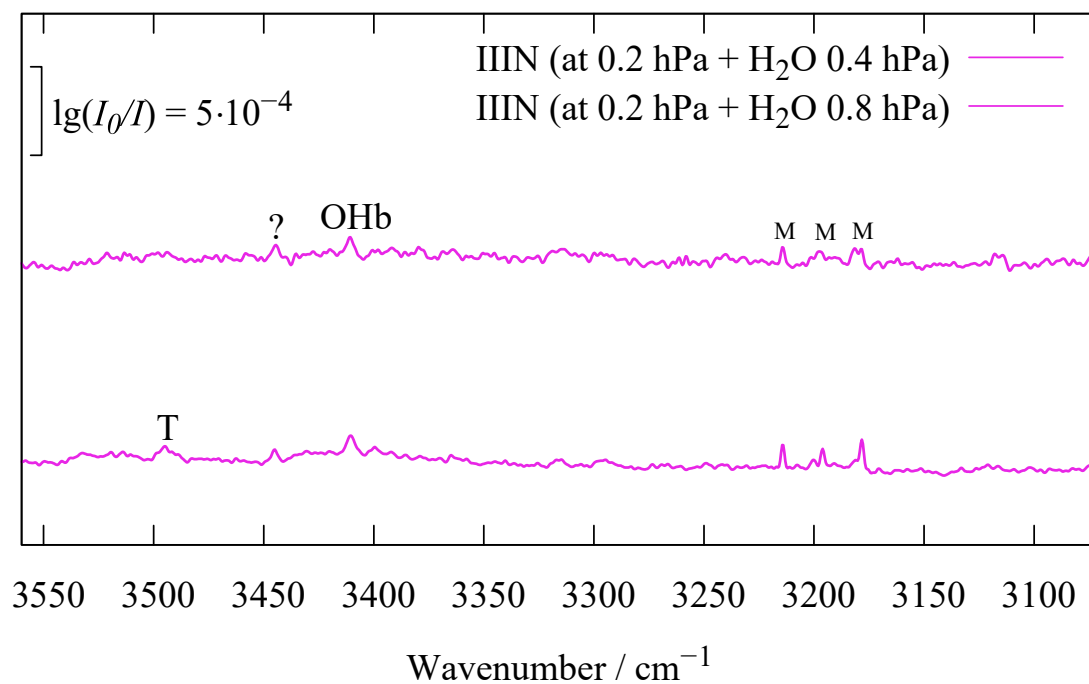


Figure S21: Spectra of the monohydrate WA and dihydrate WWA of triisopropylamine (IIIN) with two different concentrations of water. The dihydrate WWA for IIIN can be clearly separated from the heterodimer features. T is the raw dihydrate signal for indirect solvation contact.

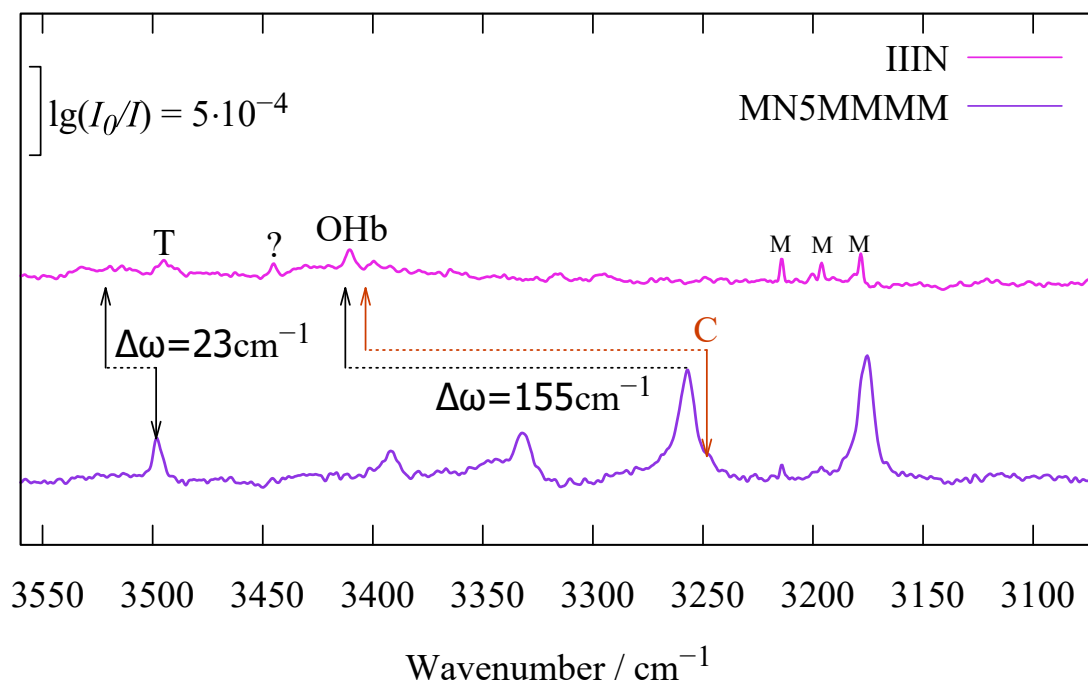


Figure S22: Spectral comparison of IIN and MN5MMMM with water. The OH stretching vibration OHb for IIN monohydrate is predicted by adding the harmonic shift 155 cm^{-1} to the raw and the centroid C position of MN5MMMM. The raw dihydrate signal for indirect solvation contact T is predicted by adding the harmonic shift 23 cm^{-1} to the raw T position of MN5MMMM.

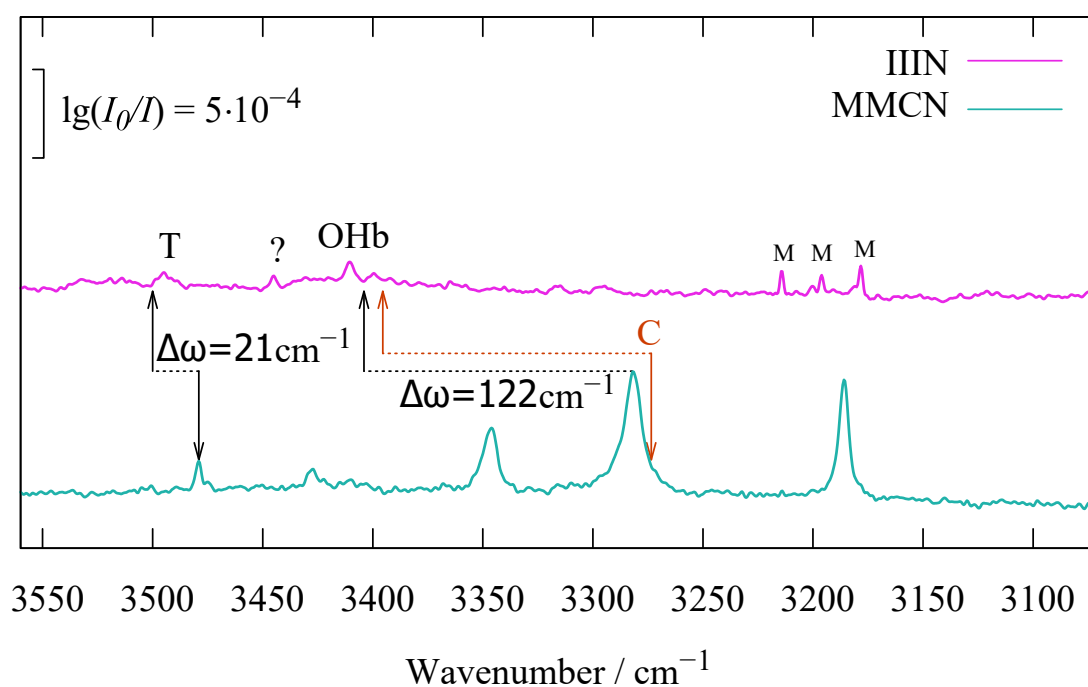


Figure S23: Spectral comparison of IIN and MMCN with water. The OH stretching vibration OHb for IIN monohydrate is predicted by adding the harmonic shift 122 cm^{-1} to the raw and the centroid C position of MMCN. The raw dihydrate signal for indirect solvation contact T is predicted by adding the harmonic shift 21 cm^{-1} to the raw T position of MMCN.

11 Example inputs for transition states

NEB scans^[15] are used to calculate the energy barrier between three EEEN conformers: EEEN1, EEEN2 and EEEN3. The structure of the transition state from the NEB scan is reoptimized again by using B3LYP-D3/def2-TZVP on ORCA 5.0.3 with the keywords shown in Table S28. The figure for the energy barrier of EEEN conformers is shown in Fig. 9 in the main text.

For convenience, an example input for the NEB scan and transition state calculation are given in Table S27 and S28.

Table S27: Example input for NEB scan in the ORCA 5.0.3 calculations at the B3LYP level of computation. In the input file, "start.xyz" is the name of the beginning conformer and "end.xyz" is the name of the ending conformer that needed to convert.^[15]

type of calculation	input
NEB scan	!NEB-CI B3LYP D3BJ abc def2-TZVP VeryTightSCF defgrid3 Mass2016 %neb NEB_End_XYZFile "start.xyz" SpringType DOF PerpSpring cosTan Tol_MaxF_CI 2.e-3 Tol_RMSF_CI 1.e-3 Tol_Scale 10.0 Local true Nimages 30 end %pal nprocs 30 end %Maxcore 3000 *xyzfile 0 1 end.xyz

Table S28: Example input for the transition state calculation in the ORCA 5.0.3 calculations at the B3LYP level of computation.^[16]

type of calculation	input
Transition state	!B3LYP D3BJ abc def2-TZVP UseSym SlowConv OptTS VeryTightOpt VeryTightSCF Freq defgrid3 Mass2016 %method SymThresh 5.0e-2 end %geom Calc_Hess true Recalc_Hess 3 ENFORCESTRICTCONVERGENCE true MaxIter 500 end %pal nprocs NUMCORES end %Maxcore 3000 *xyzfile 0 1 Start.xyz

References

- [1] H. C. Gottschalk, T. L. Fischer, V. Meyer, R. Hildebrandt, U. Schmitt, M. A. Suhm, *Instruments* **2021**, *5*, 12.
- [2] N. O. B. Lüttchwager, *Phys. Chem. Chem. Phys.* **2024**, *26*, 10120–10135.
- [3] N. O. B. Lüttchwager, *Journal of Open Source Software* **2021**, *6*, 3526.
- [4] S. Grimme, J. Antony, S. Ehrlich, H. Krieg, *J. Chem. Phys.* **2010**, *132*, 154104.
- [5] S. Grimme, S. Ehrlich, L. Goerigk, *J. Comput. Chem.* **2011**, *32*, 1456–1465.
- [6] F. Weigend, R. Ahlrichs, *Phys. Chem. Chem. Phys.* **2005**, *7*, 3297–3305.
- [7] W. Sander, S. Roy, I. Polyak, J. M. Ramirez-Angueta, E. Sanchez-Garcia, *J. Am. Chem. Soc.* **2012**, *134*, 8222–8230.
- [8] D. Leicht, M. Kaufmann, R. Schwan, J. Schäfer, G. Schwaab, M. Havenith, *J. Chem. Phys.* **2016**, *145*, 204305.
- [9] F. Neese, *Wiley Interdiscip. Rev. Comput. Mol. Sci.* **2012**, *2*, 73–78.
- [10] F. Neese, *Wiley Interdiscip. Rev. Comput. Mol. Sci.* **2022**, *12*, e1606.
- [11] M. A. Marques, M. J. Oliveira, T. Burnus, *Computer Physics Communications* **2012**, *183*, 2272–2281.
- [12] S. Lehtola, C. Steigemann, M. J. Oliveira, M. A. Marques, *SoftwareX* **2018**, *7*, 1–5.
- [13] S. Grimme, *J. Chem. Theory Comput.* **2019**, *15*, 2847–2862.
- [14] P. Pracht, F. Bohle, S. Grimme, *Phys. Chem. Chem. Phys.* **2020**, *22*, 7169–7192.
- [15] V. Ásgeirsson, B. O. Birgisson, R. Bjornsson, U. Becker, F. Neese, C. Riplinger, H. Jónsson, *Journal of Chemical Theory and Computation* **2021**, *17*, PMID: 34275279, 4929–4945.
- [16] B. Dmytro, P. Taras, I. Róbert, K. Simone, B. Ute, V. Edward, N. Frank, *Molecular Physics* **2015**, *113*, 1961–1977.

Part 2: Julia Package Fermi4x4

Contents

Introduction	F3
Finding Proper L	F4
Building a General L Matrix	F4
Finding D	F9
References	F10
Appendix: Checks for Correctness	F10
3x3 Problem	F10
4x4 Problem	F12

Part 2: Julia Package Fermi4x4

This document explains the inner workings of the Fermi4x4 package. In particular, it derives the mathematical expressions which are used in the package. Derivation of these expressions was done using Python (<https://python.org/>), Numpy (<https://numpy.org/>), and Sympy (<https://sympy.org/>) in the versions specified below.

This document is a converted Jupyter notebook (found together with the Fermi4x4 source code under <https://gitlab.gwdg.de/nluetts/fermi4x4.jl>) and therefore contains code blocks which show how exactly the mathematical expressions were derived. Note that the output of a code block is shown directly under it and it is required for the understanding of the text.

```
1 # imports
2 import sys
3
4 import numpy as np
5 import sympy as sy
6 from IPython.display import Markdown, display
7 from sympy import Matrix, cos, sin, symbols
```

```
1 # print versions, for reproducibility
2 print("Python version: ", sys.version)
3 print("Numpy version: ", np.__version__)
4 print("Sympy version: ", sy.__version__)
```

```
1 Python version: 3.11.9 | packaged by conda-forge | (main, Apr 19 2024, 18:36:13) [GCC 12.3.0]
2 Numpy version: 1.26.4
3 Sympy version: 1.12
```

```
1 def disp_eq(var, expr):
2     if type(var) == str:
3         display(sy.Eq(sy.Symbol(var), expr, evaluate=False))
4     else:
5         display(sy.Eq(var, expr, evaluate=False))
```

Introduction

This Julia package provides functions to solve a particular type of inverse eigenvalue problem that comes up in vibrational spectroscopy: Given a set 3 to 4 experimental band positions and associated intensities, where it is assumed that the excited states perturb each other due to anharmonic resonance, find a set of *deperturbed* wavenumbers and coupling elements that are compatible with the experimental data.

In terms of linear algebra, the problem can be formulated as follows:

$$\mathbf{D} = \mathbf{L}\mathbf{F}\mathbf{L}^T$$

Here, \mathbf{D} is a symmetric 3x3 or 4x4 matrix that holds deperturbed band positions (diagonal elements) and coupling elements (off-diagonal elements). \mathbf{F} is a diagonal matrix made up of the eigenvalues of \mathbf{D} , which are the observed (perturbed) band positions. \mathbf{L} is an orthonormal matrix built from the eigenvectors of \mathbf{D} and contains information about the experimental intensities. This intensity information is, however, not enough to fully specify \mathbf{L} . Thus, to solve the problem, several assumptions are made:

- There is only one deperturbed state with a relevant ground state transition moment, the "bright state", while the remaining 2 to 3 deperturbed "dark states" have negligible transition moments.
- Some of the coupling elements are *constrained* to certain values

With \mathbf{F} being available from the experiment, the task is to find proper \mathbf{L} that yield coupling elements in the \mathbf{D} matrix that fulfill the given constraints. One row vector of \mathbf{L} is derived from experimental intensities. Finding the remaining elements is done *via* a minimization step.

Note that it is also possible to solve a 2x2 (Fermi resonance) problem by setting the intensity of one band put into the 3x3 problem to zero.

Finding Proper \mathbf{L}

The matrix \mathbf{L} is orthonormal, of size 3x3 or 4x4, and has one normalized row vector of the form:

$$\vec{l}_1 = [\sqrt{I_1}, \sqrt{I_2}, \sqrt{I_3}, (\sqrt{I_4})] = [b_1, b_2, b_3, b_4]$$

The elements I_i are experimental intensities and are scaled so that the vector \vec{l}_1 is of length 1.

The experimental intensities are not sufficient to fully specify \mathbf{L} : An orthonormal $n \times n$ matrix has $n(n - 1)/2$ degrees of freedom (DOF), yielding 3 DOF for the 3x3 and 6 DOF for the 4x4 matrix. With the experimental intensities, 2 (3x3) or 3 (4x4) of these DOF are already constrained (one DOF less than the number of intensities, because the row vector shown above is normalized). This leaves **1 degree of freedom for the 3x3 problem and 3 degrees of freedom for 4x4 problem.**

To solve the inverse eigenvalue problem, the 1 (3) remaining DOF of the \mathbf{L} matrix are varied such that the off-diagonal elements of the \mathbf{D} matrix stay true to certain constraints provided by the user, e.g. couplings among dark states may be forced to zero. However, we have yet to define what these degrees of freedom actually are.

Building a General \mathbf{L} Matrix

There are several ways to set up the degrees of freedom in a general expression, but here we derive an expression for \mathbf{L} as follows: From experimental intensities, we have one row vector \vec{l}_1 given above. Additionally, we use the fact that if \mathbf{A} is an orthonormal matrix and \mathbf{B} is an orthonormal matrix and

$$\mathbf{C} = \begin{pmatrix} 1 & 0 \\ 0 & \mathbf{B} \end{pmatrix}$$

then $\mathbf{L} = \mathbf{C} \times \mathbf{A}$ is an orthonormal matrix with the same first row as \mathbf{A} [1]. This allows us to generate different valid (orthonormal) \mathbf{L} matrices while keeping the known row vector from the experimental data.

For \mathbf{A} we need an "initial guess". For \mathbf{B} for the 3x3 problem we choose the general 2x2 rotation matrix in 2 dimensions (in the xy plane) which then constrains, *via* its rotation angle θ , the one remaining DOF of $\mathbf{L}_{3 \times 3}$ when one normal row vector is already given:

```
1 # Rotation in xy plane in 2D
2 def get_B_3x3():
3     theta = symbols("theta")
4     R = Matrix([[cos(theta), -sin(theta)], [sin(theta), cos(theta)]])
5     return R
6
7
8 B_3x3 = get_B_3x3()
9
10 disp_eq("B_{3}\times3", B_3x3)
```

$$B_{3 \times 3} = \begin{bmatrix} \cos(\theta) & -\sin(\theta) \\ \sin(\theta) & \cos(\theta) \end{bmatrix}$$

For \mathbf{B} for the 4x4 problem, we choose a general 3x3 rotation matrix in 3 dimensions which constrains the 3 remaining DOF of $\mathbf{L}_{4 \times 4}$ *via* its rotation angles around the x , y and z axes:

```
1 # Rotation in yz plane in 3D
2 def Rx():
3     tx = symbols("theta_x")
4     R = Matrix([[1, 0, 0], [0, cos(tx), -sin(tx)], [0, sin(tx), cos(tx)]])
5     return R
6
7
8 # Rotation in xz plane in 3D
9 def Ry():
10    ty = symbols("theta_y")
11    R = Matrix([[cos(ty), 0, sin(ty)], [0, 1, 0], [-sin(ty), 0, cos(ty)]])
12    return R
13
14
15 # Rotation in xy plane in 3D
16 def Rz():
17    tz = symbols("theta_z")
```

Part 2: Julia Package Fermi4x4

```

18     R = Matrix([[cos(tz), -sin(tz), 0], [sin(tz), cos(tz), 0], [0, 0, 1]])
19     return R
20
21
22 # Rotation around all 3 axes in 3D
23 def get_B_4x4():
24     return Rx() * Ry() * Rz()
25
26
27 B_4x4 = get_B_4x4()
28
29 disp_eq("B_{4\\times4}", B_4x4)

```

$$B_{4 \times 4} = \begin{bmatrix} \cos(\theta_y) \cos(\theta_z) & -\sin(\theta_z) \cos(\theta_y) & \sin(\theta_y) \\ \sin(\theta_x) \sin(\theta_y) \cos(\theta_z) + \sin(\theta_z) \cos(\theta_x) & -\sin(\theta_x) \sin(\theta_y) \sin(\theta_z) + \cos(\theta_x) \cos(\theta_z) & -\sin(\theta_x) \cos(\theta_y) \\ \sin(\theta_x) \sin(\theta_z) - \sin(\theta_y) \cos(\theta_x) \cos(\theta_z) & \sin(\theta_x) \cos(\theta_z) + \sin(\theta_y) \sin(\theta_z) \cos(\theta_x) & \cos(\theta_x) \cos(\theta_y) \end{bmatrix}$$

For the 3x3 problem, we construct the initial orthonormal matrix \mathbf{A} starting with the vector \vec{l}_1 , finding an orthogonal vector \vec{l}_2 by setting $z_2 = 0$ (an arbitrary choice) and then calculating the cross product of \vec{l}_1 and \vec{l}_2 to find \vec{l}_3 :

```

1  def get_A_3x3():
2     a1, a2 = symbols("a1, a2")
3     b1, b2, b3 = symbols("b1, b2, b3")
4     # find elements of l_2
5     a1, a2 = sy.solve([a1**2 + a2**2 - 1, a1 * b1 + a2 * b2], a1, a2)[0]
6     v1 = sy.Matrix([b1, b2, b3])
7     v2 = sy.Matrix([a1, a2, 0])
8     v3 = v2.cross(v1)
9     return Matrix([v1, v2, v3]).reshape(3, 3)
10
11
12 A_3x3 = get_A_3x3()
13
14 disp_eq("A_{3\\times3}", A_3x3)

```

$$A_{3 \times 3} = \begin{bmatrix} b_1 & b_2 & b_3 \\ -b_2 \sqrt{\frac{1}{b_1^2 + b_2^2}} & b_1 \sqrt{\frac{1}{b_1^2 + b_2^2}} & 0 \\ b_1 b_3 \sqrt{\frac{1}{b_1^2 + b_2^2}} & b_2 b_3 \sqrt{\frac{1}{b_1^2 + b_2^2}} & -b_1^2 \sqrt{\frac{1}{b_1^2 + b_2^2}} - b_2^2 \sqrt{\frac{1}{b_1^2 + b_2^2}} \end{bmatrix}$$

For the 4x4 problem, we construct the initial orthonormal matrix \mathbf{A} using a trick involving quaternions. In this way, the matrix is constructed by Sympy automatically:

```
1 A_4x4 = sy.Quaternion("b1", "b2", "b3", "b4").product_matrix_left.transpose()
2
3 disp_eq("A_{4\\times4}", A_4x4)
```

$$A_{4 \times 4} = \begin{bmatrix} b_1 & b_2 & b_3 & b_4 \\ -b_2 & b_1 & b_4 & -b_3 \\ -b_3 & -b_4 & b_1 & b_2 \\ -b_4 & b_3 & -b_2 & b_1 \end{bmatrix}$$

We can check for orthonormality to verify that this is a valid initial \mathbf{A} matrix (further such checks for correctness are included below):

```
1 AA_t = sy.simplify(A_4x4 * A_4x4.transpose())
2
3 disp_eq(sy.Symbol("A_{4\\times4}") * sy.Symbol("A_{4\\times4}") ** sy.Symbol("T"), AA_t)
```

$$A_{4 \times 4} A_{4 \times 4}^T = \begin{bmatrix} b_1^2 + b_2^2 + b_3^2 + b_4^2 & 0 & 0 & 0 \\ 0 & b_1^2 + b_2^2 + b_3^2 + b_4^2 & 0 & 0 \\ 0 & 0 & b_1^2 + b_2^2 + b_3^2 + b_4^2 & 0 \\ 0 & 0 & 0 & b_1^2 + b_2^2 + b_3^2 + b_4^2 \end{bmatrix}$$

This is OK, since \vec{l}_1 is normalized ($|\vec{l}_1| = \sum b_i^2 = 1$).

With both \mathbf{A} and \mathbf{B} in place, we can derive general expressions for $\mathbf{L}_{3 \times 3}$ and $\mathbf{L}_{4 \times 4}$:

```
1 def get_C_3x3():
2     C = sy.eye(3)
3     C[1:3, 1:3] = get_B_3x3()
4     return C
5
6
7 C_3x3 = get_C_3x3()
8
```

Part 2: Julia Package Fermi4x4

```

9 L_3x3 = C_3x3 * A_3x3
10 L_3x3.simplify()
11 disp_eq("L_{3\\times3}", L_3x3)

```

$$L_{3 \times 3} = \begin{bmatrix} b_1 & b_2 & b_3 \\ - (b_1 b_3 \sin(\theta) + b_2 \cos(\theta)) \sqrt{\frac{1}{b_1^2 + b_2^2}} & (b_1 \cos(\theta) - b_2 b_3 \sin(\theta)) \sqrt{\frac{1}{b_1^2 + b_2^2}} & (b_1^2 + b_2^2) \sqrt{\frac{1}{b_1^2 + b_2^2}} \sin(\theta) \\ (b_1 b_3 \cos(\theta) - b_2 \sin(\theta)) \sqrt{\frac{1}{b_1^2 + b_2^2}} & (b_1 \sin(\theta) + b_2 b_3 \cos(\theta)) \sqrt{\frac{1}{b_1^2 + b_2^2}} & - (b_1^2 + b_2^2) \sqrt{\frac{1}{b_1^2 + b_2^2}} \cos(\theta) \end{bmatrix}$$

```

1 def get_C_4x4():
2     C = sy.eye(4)
3     C[1:4, 1:4] = get_B_4x4()
4     return C
5
6
7 C_4x4 = get_C_4x4()
8
9 L_4x4 = C_4x4 * A_4x4
10 L_4x4.simplify()
11
12 for i in range(0, 4):
13     for j in range(0, 4):
14         disp_eq(f"L_{{4\\times4\\,({i+1}\\,\\,{{j+1}})}}", L_4x4[i, j])

```

$$L_{4 \times 4}(1, 1) = b_1$$

$$L_{4 \times 4}(1, 2) = b_2$$

$$L_{4 \times 4}(1, 3) = b_3$$

$$L_{4 \times 4}(1, 4) = b_4$$

$$L_{4 \times 4}(2, 1) = -b_2 \cos(\theta_y) \cos(\theta_z) + b_3 \sin(\theta_z) \cos(\theta_y) - b_4 \sin(\theta_y)$$

$$L_{4 \times 4}(2, 2) = b_1 \cos(\theta_y) \cos(\theta_z) + b_3 \sin(\theta_y) + b_4 \sin(\theta_z) \cos(\theta_y)$$

$$L_{4 \times 4}(2, 3) = -b_1 \sin(\theta_z) \cos(\theta_y) - b_2 \sin(\theta_y) + b_4 \cos(\theta_y) \cos(\theta_z)$$

$$L_{4 \times 4}(2, 4) = b_1 \sin(\theta_y) - b_2 \sin(\theta_z) \cos(\theta_y) - b_3 \cos(\theta_y) \cos(\theta_z)$$

$$L_{4 \times 4}(3, 1) = -b_2 (\sin(\theta_x) \sin(\theta_y) \cos(\theta_z) + \sin(\theta_z) \cos(\theta_x)) + b_3 (\sin(\theta_x) \sin(\theta_y) \sin(\theta_z) - \cos(\theta_x) \cos(\theta_z)) + b_4 \sin(\theta_x) \cos(\theta_y)$$

$$L_{4 \times 4}(3, 2) = b_1 (\sin(\theta_x) \sin(\theta_y) \cos(\theta_z) + \sin(\theta_z) \cos(\theta_x)) - b_3 \sin(\theta_x) \cos(\theta_y) + b_4 (\sin(\theta_x) \sin(\theta_y) \sin(\theta_z) - \cos(\theta_x) \cos(\theta_z))$$

$$L_{4 \times 4}(3, 3) = -b_1 (\sin(\theta_x) \sin(\theta_y) \sin(\theta_z) - \cos(\theta_x) \cos(\theta_z)) + b_2 \sin(\theta_x) \cos(\theta_y) + b_4 (\sin(\theta_x) \sin(\theta_y) \cos(\theta_z) + \sin(\theta_z) \cos(\theta_x))$$

$$L_{4 \times 4}(3, 4) = -b_1 \sin(\theta_x) \cos(\theta_y) - b_2 (\sin(\theta_x) \sin(\theta_y) \sin(\theta_z) - \cos(\theta_x) \cos(\theta_z)) - b_3 (\sin(\theta_x) \sin(\theta_y) \cos(\theta_z) + \sin(\theta_z) \cos(\theta_x))$$

$$L_{4 \times 4}(4, 1) = -b_2 (\sin(\theta_x) \sin(\theta_z) - \sin(\theta_y) \cos(\theta_x) \cos(\theta_z)) - b_3 (\sin(\theta_x) \cos(\theta_z) + \sin(\theta_y) \sin(\theta_z) \cos(\theta_x)) - b_4 \cos(\theta_x) \cos(\theta_y)$$

$$L_{4 \times 4}(4, 2) = b_1 (\sin(\theta_x) \sin(\theta_z) - \sin(\theta_y) \cos(\theta_x) \cos(\theta_z)) + b_3 \cos(\theta_x) \cos(\theta_y) - b_4 (\sin(\theta_x) \cos(\theta_z) + \sin(\theta_y) \sin(\theta_z) \cos(\theta_x))$$

$$L_{4 \times 4}(4, 3) = b_1 (\sin(\theta_x) \cos(\theta_z) + \sin(\theta_y) \sin(\theta_z) \cos(\theta_x)) - b_2 \cos(\theta_x) \cos(\theta_y) + b_4 (\sin(\theta_x) \sin(\theta_z) - \sin(\theta_y) \cos(\theta_x) \cos(\theta_z))$$

$$L_{4 \times 4}(4, 4) = b_1 \cos(\theta_x) \cos(\theta_y) + b_2 (\sin(\theta_x) \cos(\theta_z) + \sin(\theta_y) \sin(\theta_z) \cos(\theta_x)) - b_3 (\sin(\theta_x) \sin(\theta_z) - \sin(\theta_y) \cos(\theta_x) \cos(\theta_z))$$

Finding **D**

The matrices $L_{3 \times 3}$ and $L_{4 \times 4}$ are hard-coded into Fermi4x4. The parameter(s) $\theta_{(x,y,z)}$ are/is optimized iteratively to find an appropriate matrix **D** that stays true to user set constraints (such as some coupling elements being zero). This is done by minimizing a loss function which depends on the type of constraints enforced on **D**. For the simple case of some coupling elements set to zero, the loss function is simply the square root of the sum of squared deviations from zero.

References

[1] This is analogous to: Angina Seng (<https://math.stackexchange.com/users/436618/angina-seng>), Answer to Question "Constructing a 4×4 orthogonal matrix having $\frac{1}{2}(1, 1, 1, 1)$ as its first row" at <https://math.stackexchange.com/a/2241474> (2017-04-19)

The PDF-export of this notebook was prepared using the Eisvogel pandoc LaTeX template (<https://github.com/Wandmalfarbe/pandoc-latex-template>).

Appendix: Checks for Correctness

3x3 Problem

Check orthonormality of B_3x3:

```
1 sy.simplify(B_3x3 * B_3x3.transpose()) # OK
```

$$\begin{bmatrix} 1 & 0 \\ 0 & 1 \end{bmatrix}$$

Check orthonormality of A_3x3:

```
1 sy.simplify(A_3x3 * A_3x3.transpose()) # OK, since l_1 normalized and  $\sum b_i^2 = 1$ 
```

$$\begin{bmatrix} b_1^2 + b_2^2 + b_3^2 & 0 & 0 \\ 0 & 1 & 0 \\ 0 & 0 & b_1^2 + b_2^2 + b_3^2 \end{bmatrix}$$

Check orthonormality of L_3x3:

```
1 LLt_3x3 = sy.simplify(L_3x3 * L_3x3.transpose())
2 LLt_3x3
```

$$\begin{bmatrix} b_1^2 + b_2^2 + b_3^2 & 0 & 0 \\ 0 & b_1^2 \sin^2(\theta) + b_2^2 \sin^2(\theta) + b_3^2 \sin^2(\theta) + \cos^2(\theta) & \frac{(-b_1^2 - b_2^2 - b_3^2 + 1) \sin(2\theta)}{2} \\ 0 & \frac{(-b_1^2 - b_2^2 - b_3^2 + 1) \sin(2\theta)}{2} & b_1^2 \cos^2(\theta) + b_2^2 \cos^2(\theta) + b_3^2 \cos^2(\theta) + \sin^2(\theta) \end{bmatrix}$$

Since it is not obvious that `LLt_3x3` is the identity matrix, we check using random numeric examples:

```

1 def random_input_3x3():
2     l1 = np.random.random(3)
3     N = np.square(l1).sum()
4     l1 /= np.sqrt(N) # normalize row vector l1
5     theta = np.random.random() * 2 * np.pi
6     return dict(b1=l1[0], b2=l1[1], b3=l1[2], theta=theta)
7
8
9 random_input_3x3() # one example input

```

```

1 {'b1': 0.5115226730713363,
2  'b2': 0.7444348247274318,
3  'b3': 0.42914024125802147,
4  'theta': 0.651800984492223}

```

```

1 LLt_3x3.subs(random_input_3x3()) # one evaluation of an example input

```

$$\begin{bmatrix} 1.0 & 0 & 0 \\ 0 & 1.0 & -5.27174402048658 \cdot 10^{-17} \\ 0 & -5.27174402048658 \cdot 10^{-17} & 1.0 \end{bmatrix}$$

```

1 # checking orthonormality of L_3x3 numerically
2
3 np.random.seed(1)
4
5 for _ in range(1000): # 1000 random tries
6     LLt = LLt_3x3.subs(random_input_3x3())
7     assert abs(LLt[0, 0]) - 1 < 1e-15
8     assert abs(LLt[1, 1]) - 1 < 1e-15
9     assert abs(LLt[2, 2]) - 1 < 1e-15
10    assert abs(LLt[0, 1]) < 1e-15
11    assert abs(LLt[0, 2]) < 1e-15
12    assert abs(LLt[1, 2]) < 1e-15

```

4x4 Problem

Check orthonormality of B_4x4:

```
1 sy.simplify(B_4x4 * B_4x4.transpose()) # OK
```

$$\begin{bmatrix} 1 & 0 & 0 \\ 0 & 1 & 0 \\ 0 & 0 & 1 \end{bmatrix}$$

Check orthonormality of A_4x4:

```
1 sy.simplify(A_4x4 * A_4x4.transpose()) # OK, since l_1 normalized and  $\sum b_i^2 = 1$ 
```

$$\begin{bmatrix} b_1^2 + b_2^2 + b_3^2 + b_4^2 & 0 & 0 & 0 \\ 0 & b_1^2 + b_2^2 + b_3^2 + b_4^2 & 0 & 0 \\ 0 & 0 & b_1^2 + b_2^2 + b_3^2 + b_4^2 & 0 \\ 0 & 0 & 0 & b_1^2 + b_2^2 + b_3^2 + b_4^2 \end{bmatrix}$$

Check orthonormality of L_4x4:

```
1 sy.simplify(L_4x4 * L_4x4.transpose()) # OK, since l_1 normalized and  $\sum b_i^2 = 1$ 
```

$$\begin{bmatrix} b_1^2 + b_2^2 + b_3^2 + b_4^2 & 0 & 0 & 0 \\ 0 & b_1^2 + b_2^2 + b_3^2 + b_4^2 & 0 & 0 \\ 0 & 0 & b_1^2 + b_2^2 + b_3^2 + b_4^2 & 0 \\ 0 & 0 & 0 & b_1^2 + b_2^2 + b_3^2 + b_4^2 \end{bmatrix}$$

Part 3: Data Evaluation Notebook (Deperturbation)

Introduction

This document is a converted Jupyter notebook and therefore contains code blocks alongside some explanatory running text. The code shows how coupling elements and deperturbed wavenumbers of dark states, as discussed in Section 4.4 of the main paper, were derived. If a code block produces some output, the output is shown directly under it. Much of this notebook is just function definitions to run the data evaluation across all data sets, using the Julia package `Fermix4x4` (ESI Section 2). The functions are documented with comments and/or "docstrings" (multi line strings enclosed in `"""` directly above the associated function definition). The main output of the notebook is a table of all required deperturbed positions/coupling elements (shown in the notebook and stored in `fermi_analysis_results.csv`). Also, plots that visualize the resulting deperturbed positions together with the spectra and input intensities/band positions are shown.

The notebook and the associated files are available from the GRO.data repository referenced in the main text (<https://doi.org/10.25625/KRTNYQ>). It can be run in a container via Podman (<https://podman.io>). To build the container with podman, use the command line and run:

```
podman build --tag amine-water-fermi-analysis -f Dockerfile
```

The produced image is tagged with `amine-water-fermi-analysis`, so we run the container from this image:

```
podman run --rm --publish 8888:8888 --volume $(pwd):/home/jovyan/work:z --users=keep-id amine-water-fermi-analysis:latest
```

(Tested using a Linux PC running Fedora 41. Note that the commands must be executed from within the folder containing the `Dockerfile`. Building and running with Docker, <https://www.docker.com/>, should also work, but is untested.)

Analysis

Preamble:

```
1 import Pkg
2 Pkg.activate(".")
```

```
1 Activating project at `~/work`
```


Part 3: Data Evaluation Notebook (Deperturbation)

```
1 # uncomment to install matching version of Fermi4x4 package
2 # (pinned via git commit SHA, keyword `rev`)
3 # Pkg.add(Pkg.PackageSpec(;url = "https://gitlab.gwdg.de/nluetts/fermi4x4.jl", rev = "b2ddda13812d77f4334de309b1c5636c19660952"))
```

```
1 using Fermi4x4
2 using Fermi4x4: ±, select_valid
3 using Markdown
4 using MonteCarloMeasurements: Particles, pmean, pstd
5 using PrettyTables
6 using Printf
7 using Random: seed!
8
9 seed!(42);
```

Define constants and helper functions:

```
1 # overwrite Fermi4x4 default behavior
2 Fermi4x4.RETRIES = 100
3 Fermi4x4.CONV_THRES = 1e-7
4
5 # raw input data, provided through a CSV file containing all
6 # required experimental band centers and intensities (and their
7 # uncertainties)
8 RAW_LINES = readlines("amines_band_center_and_intensity.csv")[2:end, :]
9 # labels of all measured substances
10 LABELS = [ "MN4", "MN5", "MNSMMMM", "N555", "MMEN", "MMIN", "MMCN", "MMTN" ]
11
12 """
13 Extract band positions and intensities from RAW_LINES for a specific substance.
14 """
15 function extract_data(label)
16     selected_rows = filter(row -> split(split(row, ',')[1], '_')[1] == label, RAW_LINES)
17     getcol(i) = [parse(Float64, split(row, ',')[i]) for row in selected_rows]
18     wavenumbers = [x ± ux for (x, ux) in zip(getcol(2), getcol(3))]
19     intensities = [x ± ux for (x, ux) in zip(getcol(4), getcol(5))]
20     # account for wavenumber dependence of integrated absorption coefficient:
21     # integral of absorption coefficient ~ transition moment2 × wavenumber
22     # (JM Hollas, "Modern Spectroscopy", 4th Ed., Wiley, 2004. Eqn. 2.17)
23     intensities = [int/wn for (wn, int) in zip(wavenumbers, intensities)]
24     # intensities are normalized to sum to 1
25     norm = sum(intensities)
26     intensities /= norm
27
28     bands([Band(wn, int) for (wn, int) in zip(wavenumbers, intensities)]...)
29 end
30
31 """
32 Format uncertain number.
33 """
```

Part 3: Data Evaluation Notebook (Deperturbation)

```
34 function to_str(val, unc)
35     udigits = -log10(unc) |> ceil |> Int
36     vdigits = -log10(val) |> ceil |> Int
37     if round(unc * 10^(udigits)) == 10
38         udigits -= 1
39     end
40     if 0 <= udigits < 5
41         @sprintf "%.*f(%i)" udigits val unc * 10^(udigits)
42     elseif udigits >= 5 && vdigits > 2 && vdigits <= udigits
43         @sprintf "%.*f(%i)e-%02i" udigits - vdigits val * 10^(vdigits) unc * 10^(udigits) vdigits
44     elseif udigits >= 5
45         @sprintf "%.*f(%i)" udigits val unc * 10^(udigits)
46     else
47         @info udigits, vdigits
48         error("Not Implemented") |> throw
49     end
50 end
51
52 to_str(x::Particles) = to_str(pmean(x), pstd(x))
53 to_str(x::String) = x;
```

Define functions to perform and display data analysis:

```
1  """
2  Calculate the center of gravity of the bands, which should be the same as the
3  deperturbed OHb wavenumber retrieved with the Fermi4x4 package and thus
4  serves as a basic sanity check that the retrieved D matrix is correct.
5  """
6  function center_of_gravity(bds)
7      wns = map(x -> x.nu, bds)
8      ints = map(x -> x.int, bds)
9      # Normalize intensities to sum to 1. To do this for the uncertain number
10     # type from MonteCarloMeasurements, we have to manipulate the individual
11     # "particles" directly.
12     for i in eachindex(ints[1].particles)
13         N = sum(int.particles[i] for int in ints)
14         for int in ints
15             int.particles[i] /= N
16         end
17     end
18     wns .* ints |> sum
19 end
20
21 """
22 Solve the 4x4 problem (model C), forcing the coupling element of the dark states
23 (state 2, 3, and 4) to zero.
24 """
25 function deperturb_4x4(bds)
26     cpls = ucouplings_4x4()
27     uncouple!(cpls, 2, 3)
```

Part 3: Data Evaluation Notebook (Deperturbation)

```
28     uncouple!(cpls, 2, 4)
29     uncouple!(cpls, 3, 4)
30     solve(bds, cpls; verify=true, show_verify=true)
31 end
32
33
34 """
35 Solve the 3x3 problem (model B), forcing the coupling element of the dark states
36 (state 2 and 3) to zero.
37 """
38 function deperturb_3x3(bds)
39     bds = bands(bds[1:3]...)
40     cpls = ucouplings_3x3()
41     uncouple!(cpls, 2, 3)
42     solve(bds, cpls; verify=false)
43 end
44
45 """
46 Solve the 2x2 problem (model A) using the 3x3 solver with on band set to zero.
47 """
48 function deperturb_2x2(bds)
49     bds = bands(Band(0.0 ± 0.0, 0.0 ± 0.0), bds[1:2]...)
50     cpls = ucouplings_3x3()
51     uncouple!(cpls, 2, 3)
52     solve(bds, cpls; verify=true, show_verify=true)
53 end
54
55
56 """
57 Evaluate models for all measurements and return the results
58 formatted in a table.
59 """
60 function run_all()
61     results = Dict{String, Any}()
62     row_labels = [
63         "Input Position OHb",
64         "Input Position b2",
65         "Input Position b20N",
66         "Input Position x0Nn",
67         "Input Intensity OHb",
68         "Input Intensity b2",
69         "Input Intensity b20N",
70         "Input Intensity x0Nn",
71         "Pos. Center of Gravity (Centroid C)",
72         "Depert. Pos. D_OHb (C)",
73         "Depert. Pos. D_b2 (C)",
74         "Depert. Pos. D_b20N (C)",
75         "Depert. Pos. D_x0Nn (C)",
76         "Coupling OHb <> b2 (C)",
77         "Coupling OHb <> b20N (C)",
78         "Coupling OHb <> x0Nn (C)",
79         "Pos. Center of Gravity (Centroid B)",
```

```

80     "Depert. Pos. D_0Hb (B)",
81     "Depert. Pos. D_b2 (B)",
82     "Depert. Pos. D_b2ON (B)",
83     "Coupling OHb <> b2 (B)",
84     "Coupling OHb <> b2ON (B)",
85     "Depert. Pos. D_b2 (A)",
86     "Depert. Pos. D_0Hb (A)",
87     "Coupling OHb <> b2 (A)",
88 ]
89 cols = [row_labels, [[] for _ in LABELS]...]
90 dat = [extract_data(label) for label in LABELS]
91 Threads.@threads for i in 1:length(LABELS)
92     bds = dat[i]
93     D4 = deperturb_4x4(bds)
94     C4 = center_of_gravity(bds)
95     D3 = deperturb_3x3(bds)
96     C3 = center_of_gravity(bds[1:3])
97     results[LABELS[i]] = (D3, D4)
98     D2 = deperturb_2x2(bds)
99     cols[i+1] = [
100         bds[2].nu, # see row_labels ...
101         bds[1].nu,
102         bds[3].nu,
103         bds[4].nu,
104         bds[2].int,
105         bds[1].int,
106         bds[3].int,
107         bds[4].int,
108         C4,
109         D4[1,1],
110         D4[2,2],
111         D4[3,3],
112         D4[4,4],
113         D4[1,2],
114         D4[1,3],
115         D4[1,4],
116         C3,
117         D3[1,1],
118         D3[2,2],
119         D3[3,3],
120         D3[1,2],
121         D3[1,3],
122         D2[3,3],
123         D2[1,1],
124         D2[1,3],
125     ]
126 end
127 io = IOBuffer();
128 pretty_table(io, hcat([to_str.(c) for c in cols]...); header = ["", LABELS...], backend=Val{:markdown});
129 results, cols, io
130 end;

```

Run analysis and display results:

```
1 results, columns, io = run_all();
2 Markdown.parse(String(take!(io)))
```

	MN4	MN5	MN5MMM	N555	MMEN	MMIN	MMCN	MMTN
Input Position OHb	3299.2(3)	3289.4(4)	3257.5(4)	3296.7(7)	3300.9(2)	3284.7(4)	3282.0(3)	3268.6(5)
Input Position b2	3190.8(8)	3188.7(9)	3176.2(3)	3193.3(4)	3191.4(3)	3187.0(3)	3186.1(2)	3180.2(3)
Input Position b2ON	3347.6(4)	3342.3(4)	3334(2)	3351.2(5)	3351.6(6)	3348.0(3)	3347.1(6)	3344.4(7)
Input Position xONn	3441(1)	3429(1)	3393.1(8)	3441(2)	3446(2)	3431(1)	3426.6(7)	3413(1)
Input Intensity OHb	0.61(3)	0.64(4)	0.40(3)	0.53(3)	0.60(3)	0.55(2)	0.51(4)	0.46(3)
Input Intensity b2	0.20(3)	0.22(4)	0.42(3)	0.28(2)	0.19(3)	0.30(2)	0.29(3)	0.38(3)
Input Intensity b2ON	0.19(3)	0.13(2)	0.17(4)	0.19(2)	0.21(2)	0.15(1)	0.20(3)	0.16(2)
Input Intensity xONn	0.03(2)	0.05(1)	0.08(1)	0.04(2)	0.02(1)	0.03(2)	0.036(9)	0.03(1)
Pos. Center of Gravity (Centroid C)	3292(5)	3281(5)	3248(5)	3284(4)	3294(4)	3270(3)	3273(4)	3252(4)
Depert. Pos. D_OHb (C)	3292(5)	3281(5)	3248(5)	3284(4)	3294(4)	3270(3)	3273(4)	3252(4)
Depert. Pos. D_b2 (C)	3214(4)	3212(4)	3214(3)	3225(3)	3213(3)	3218(2)	3216(3)	3217(2)
Depert. Pos. D_b2ON (C)	3337(1)	3334(1)	3315(4)	3338(1)	3339(1)	3336.0(9)	3331(2)	3328(3)
Depert. Pos. D_xONn (C)	3437(3)	3423(2)	3383(2)	3435(3)	3444(3)	3426(3)	3422(1)	3409(2)
Coupling OHb <> b2 (C)	46(3)	44(3)	45.4(9)	51(1)	46(3)	48.5(9)	48(2)	47.0(8)
Coupling OHb <> b2ON (C)	23(1)	22(1)	41(3)	27(1)	24(1)	29(1)	33(2)	37(2)
Coupling OHb <> xONn (C)	24(8)	30(5)	33(3)	27(7)	17(9)	26(7)	25(3)	23(7)
Pos. Center of Gravity (Centroid B)	3287(4)	3274(5)	3236(5)	3278(3)	3291(3)	3265(2)	3268(4)	3247(3)
Depert. Pos. D_OHb (B)	3287(4)	3274(5)	3236(5)	3278(3)	3291(3)	3265(2)	3268(4)	3247(3)
Depert. Pos. D_b2 (B)	3214(4)	3213(4)	3215(3)	3225(3)	3214(3)	3219(2)	3217(3)	3217(2)
Depert. Pos. D_b2ON (B)	3337(1)	3334(1)	3317(4)	3338(1)	3339(1)	3336.3(9)	3331(2)	3329(2)
Coupling OHb <> b2 (B)	46(3)	44(3)	43.9(9)	50(1)	46(3)	48.0(9)	48(2)	46.4(7)
Coupling OHb <> b2ON (B)	22(1)	21(1)	37(4)	26(1)	24(1)	27.7(9)	32(2)	35(2)
Depert. Pos. D_b2 (A)	3218(4)	3215(5)	3218(3)	3229(3)	3217(4)	3222(2)	3220(4)	3220(2)
Depert. Pos. D_OHb (A)	3272(4)	3263(5)	3216(3)	3261(3)	3275(4)	3250(2)	3248(4)	3229(2)
Coupling OHb <> b2 (A)	46(3)	44(3)	40.5(3)	49(1)	46(2)	46.7(7)	46(1)	43.9(4)

Write results to CSV file:

```

1 open("fermi_analysis_results.csv", "w") do f
2   ncols = length(columns)
3   nrows = length(columns[1])
4   write(f, "quantity,")
5   for (i, label) in enumerate(LABELS)
6     write(f, "$(label) mean,$(label) std")
7     if i == ncols - 1
8       write(f, "\n")
9     else
10      write(f, ",")
11    end
12  end
13  for i in 1:nrows
14    for j in 1:ncols
15      val = columns[j][i]
16      if val isa String
17        write(f, val)
18      else
19        mean = @sprintf "%.4f" pmean(val)
20        std = @sprintf "%.4f" pstd(val)
21        write(f, mean, ",", std)
22      end
23      if j == ncols
24        write(f, "\n")
25      else
26        write(f, ",")
27      end
28    end
29  end
30 end

```

Plot input data (spectrum as line plot, input intensities and positions as bar plot) and deperturbed positions (as histograms):

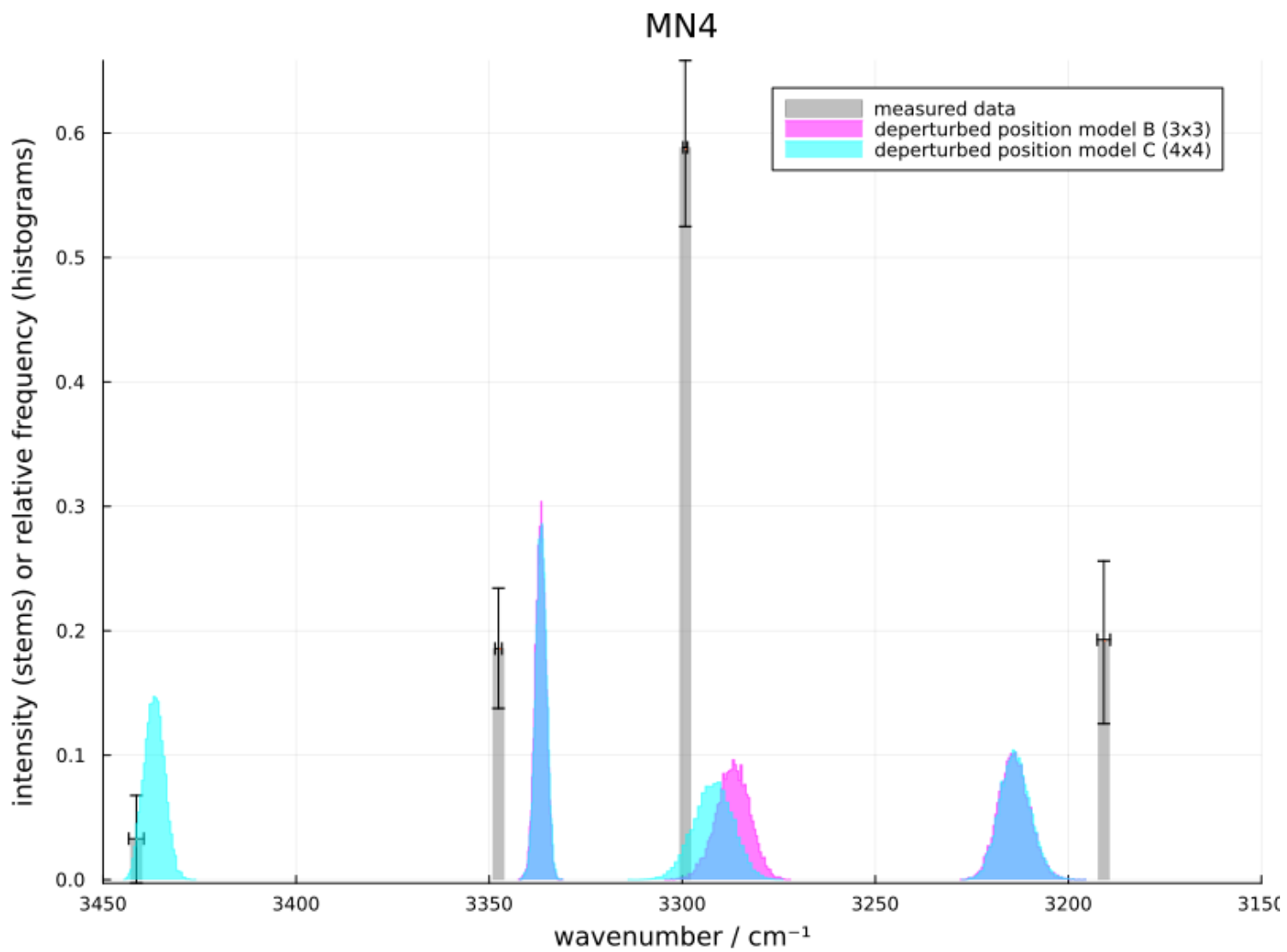
```

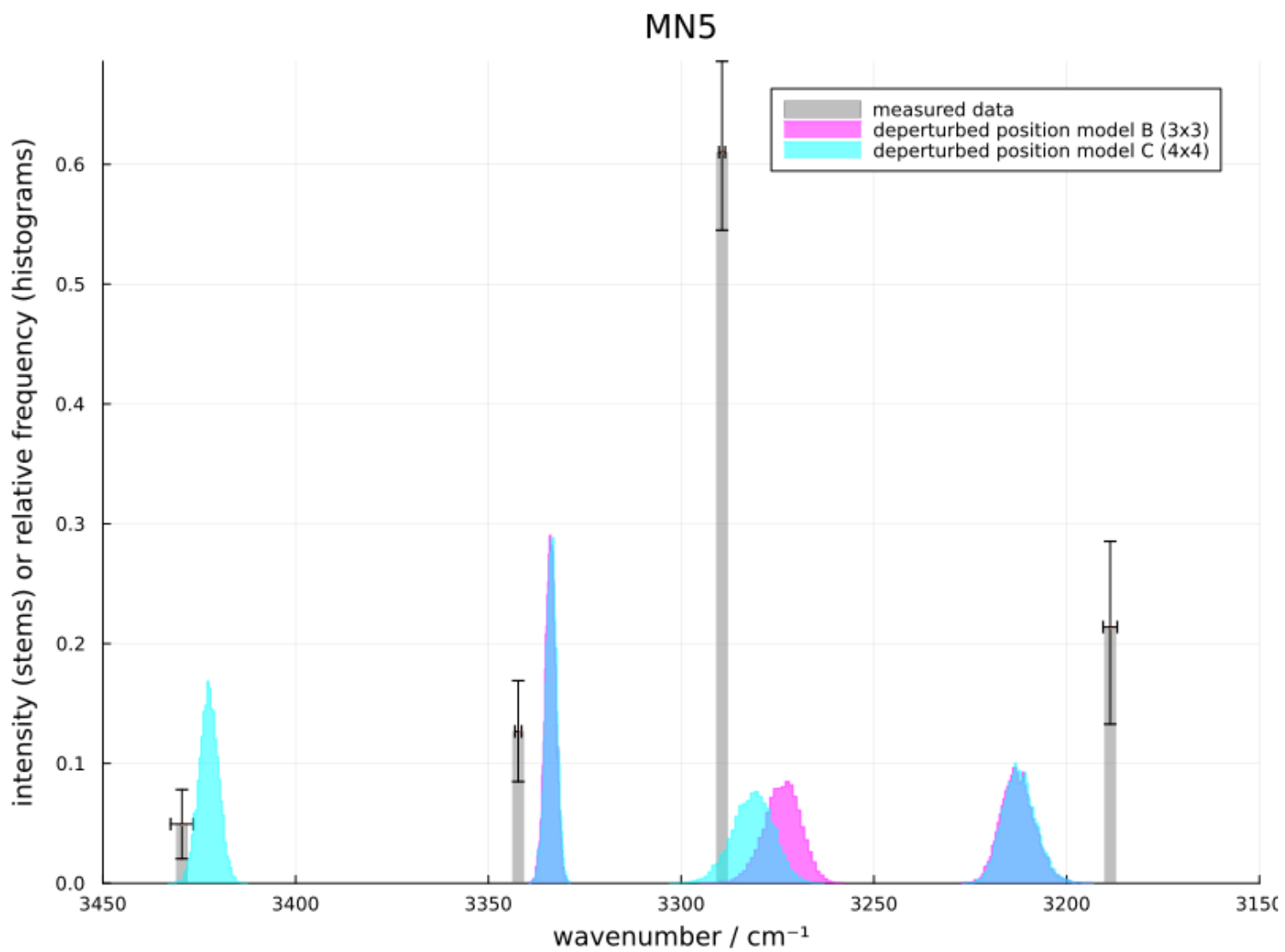
1 using Plots
2 using LinearAlgebra
3
4 function visualize(label, D3, D4)
5
6   # plot input data
7   bds = extract_data(label)
8   wns = map(x -> x.nu, bds) |> collect
9   ints = map(x -> x.int, bds) |> collect
10  plt = bar(wns .|> pmean, ints .|> pmean;
11    bar_width=3, linewidth=0.0, color=:gray,
12    label="measured data", title=label, alpha=0.5,
13    xflip=true, xlims=(3150, 3450)
14  )
15  scatter!(wns, ints; shape=:pixel, label=nothing)

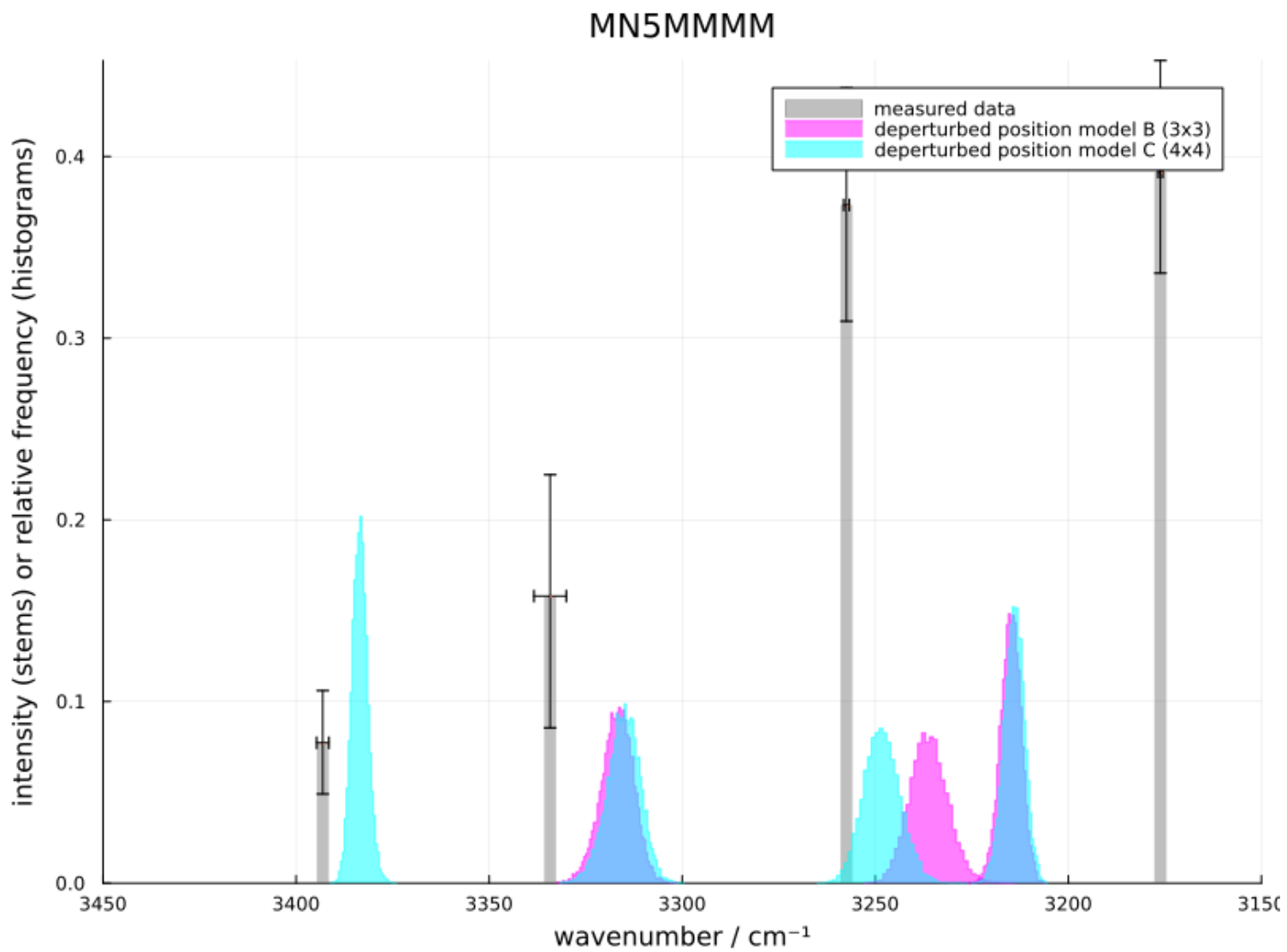
```

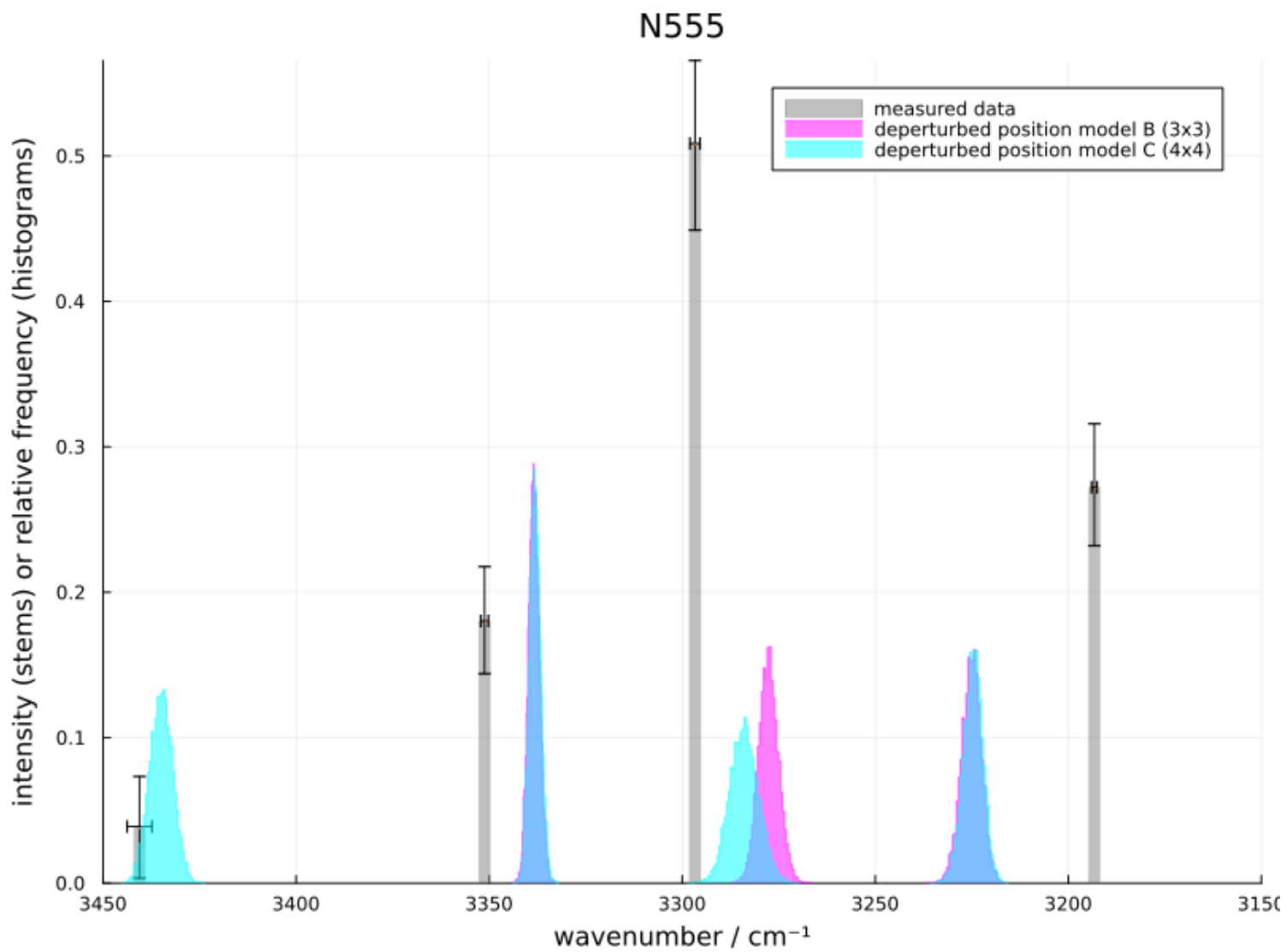
Part 3: Data Evaluation Notebook (Deperturbation)

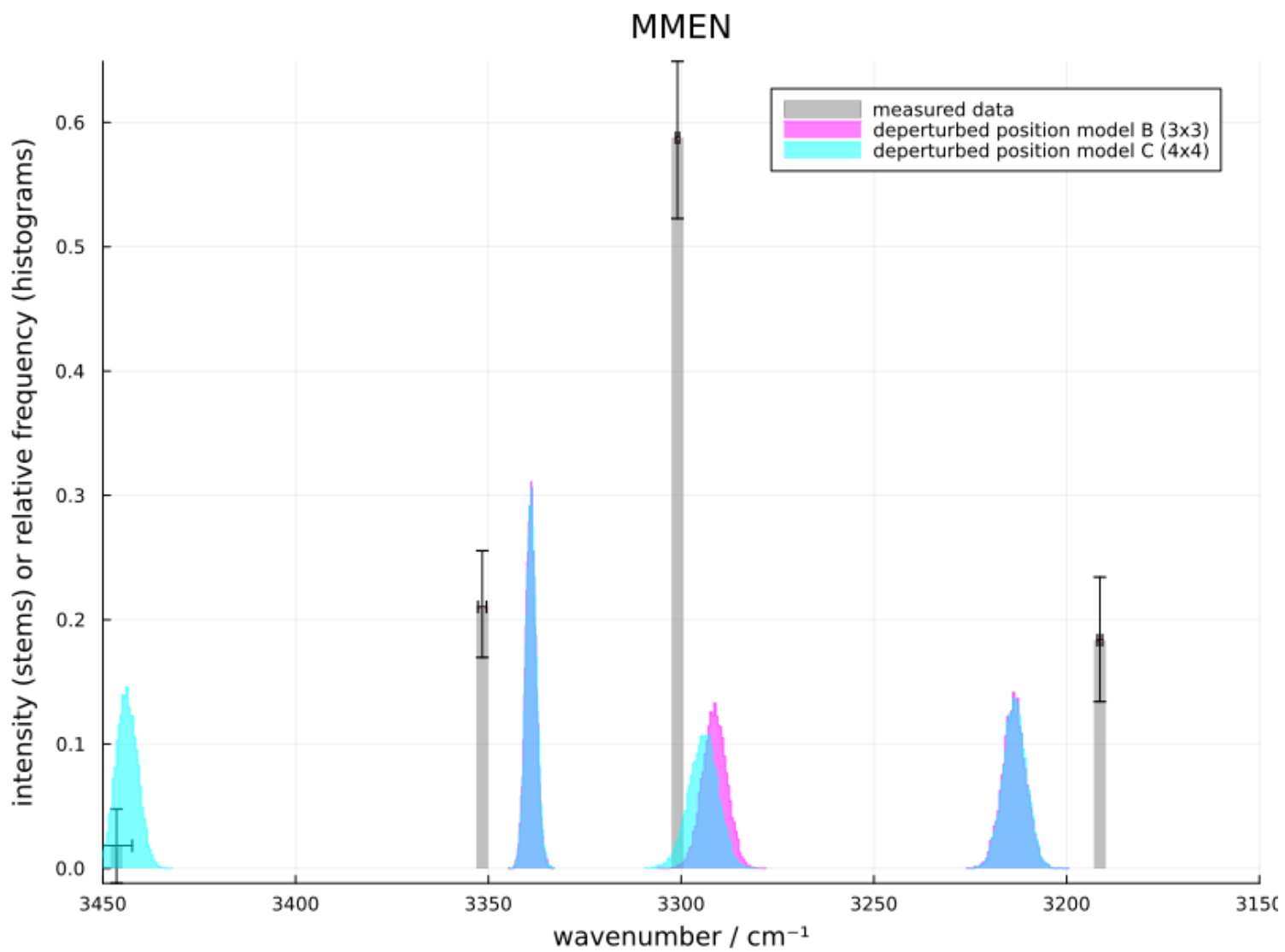
```
16
17 # plot settings array_from_fields(ints) array_from_fields(wls)
18 kw = Dict(:fill => true, :color => :magenta, :alpha => 0.5, :normalize => true, :size => (800, 600))
19
20 # plot histograms for 3x3 problem
21 for (i, p) in enumerate(diag(D3))
22     current_label = i == 1 ? "deperturbed position model B (3x3)" : nothing
23     stephist!(plt, p; kw..., normalize=true, label=current_label)
24 end
25
26 # plot histograms for 4x4 problem
27 kw[:color] = :cyan
28 for (i, p) in enumerate(diag(D4))
29     current_label = i == 1 ? "deperturbed position model C (4x4)" : nothing
30     stephist!(plt, p; kw..., normalize=true, label=current_label)
31 end
32
33 xlabel!("wavenumber /  $\mu\text{cm}^{-1}$ ")
34 ylabel!("intensity (stems) or relative frequency (histograms)")
35 end
36
37 for label in LABELS
38     D3, D4 = results[label]
39     visualize(label, D3, D4) |> display
40 end
```

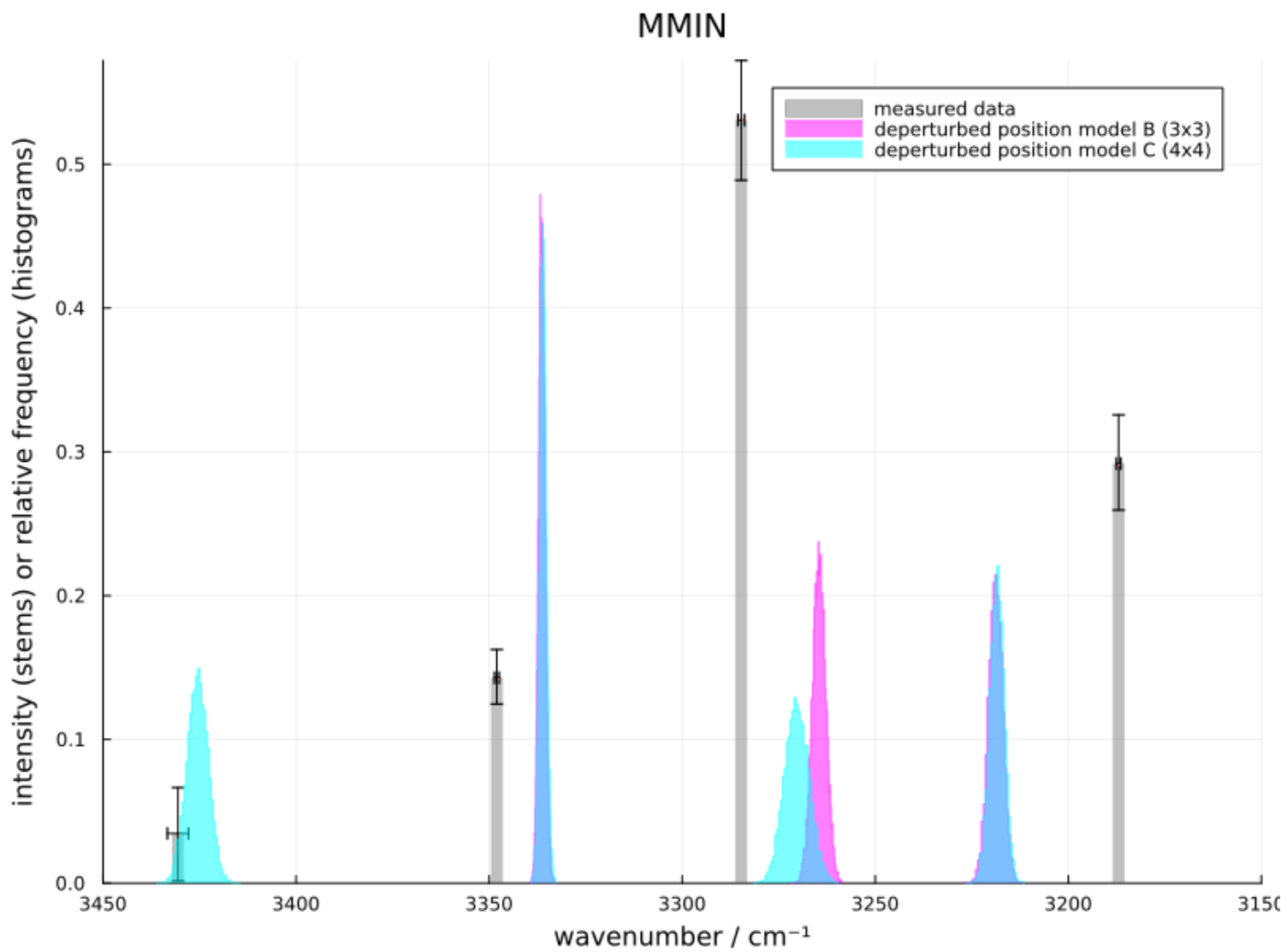


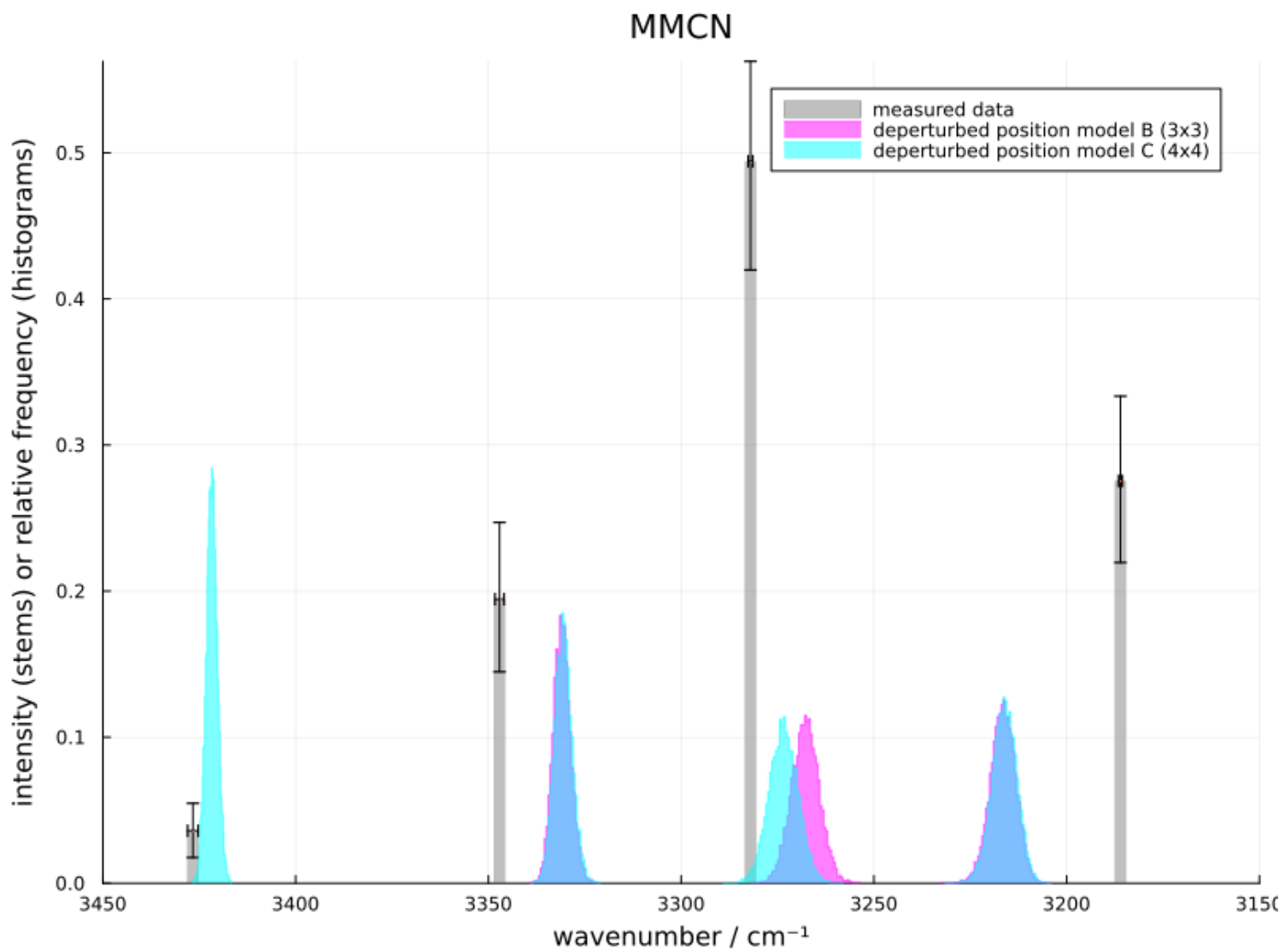


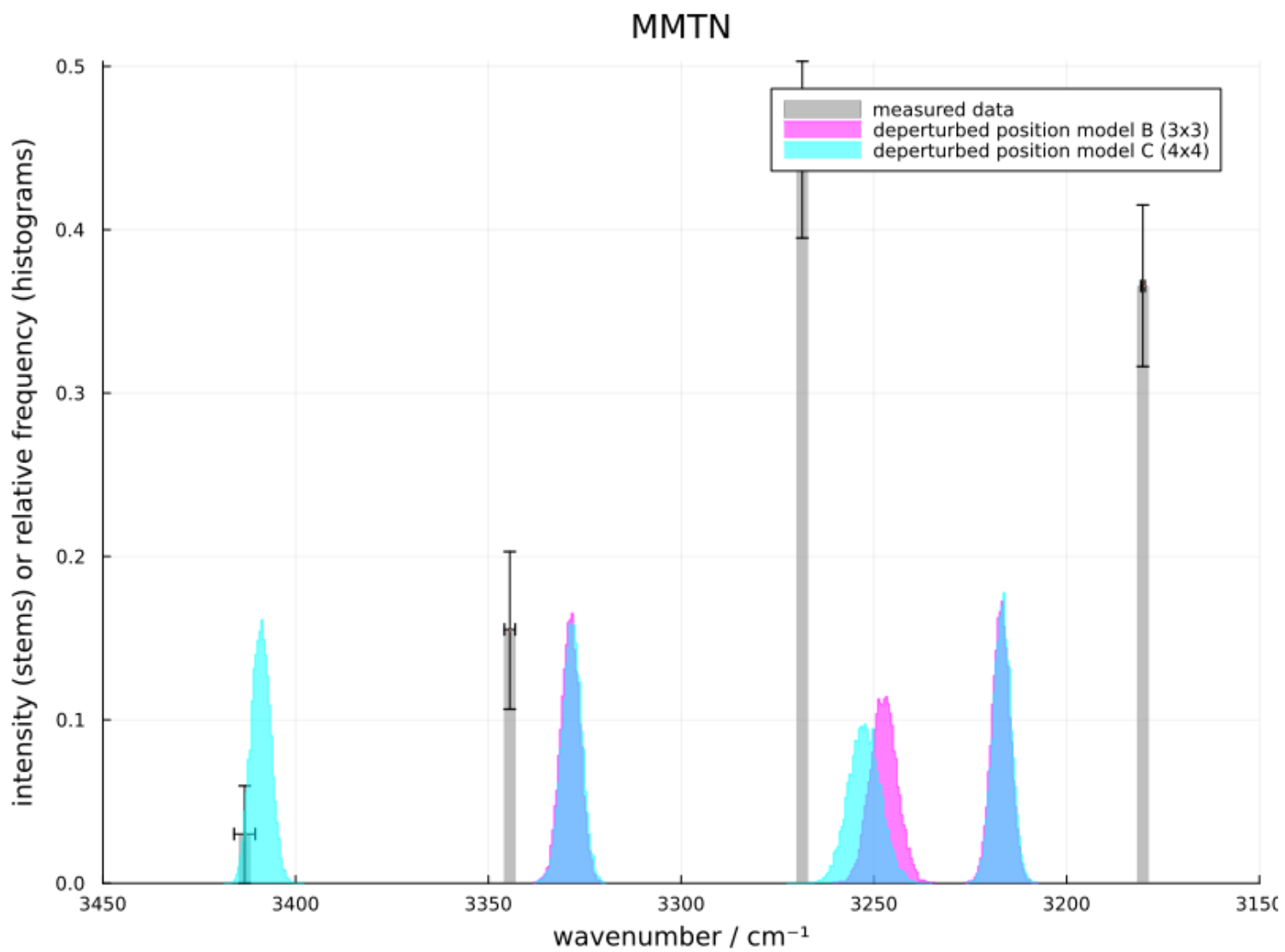












The PDF-export of this notebook was prepared using the Eisevogel pandoc LaTeX template (<https://github.com/Wandmalfarbe/pandoc-latex-template>).